Structural, Biochemical, and Functional Characterization of the Calcium Sensor Neurocalcin δ in the Inner Retinal Neurons and Its Linkage with the Rod Outer Segment Membrane Guanylate Cyclase Transduction System†

Anuradha Krishnan,‡ Venkateswar Venkataraman,‡ Ewa Fik-Rymarkiewicz, Teresa Duda, and Rameshwar K. Sharma*

The Unit of Regulatory and Molecular Biology, Departments of Cell Biology and Ophthalmology, SOM and NJMS, University of Medicine and Dentistry of New Jersey, Stratford, New Jersey 08084

Received September 10, 2003; Revised Manuscript Received November 20, 2003

ABSTRACT: This study documents the detailed biochemical, structural, and functional identity of a novel Ca^{2+}-modulated membrane guanylate cyclase transduction system in the inner retinal neurons. The guanylate cyclase is the previously characterized ROS-GC1 from the photoreceptor outer segments (PROS), and its new modulator is neurocalcin δ. At the membrane, the myristoylated form of neurocalcin δ senses submicromolar increments in free Ca^{2+}, binds to its specific ROS-GC1 domain, and stimulates the cyclase. Neurocalcin δ is not present in PROS, indicating the absence of the pathway in the outer segments and the dissociation of its linkage with phototransduction. Thus, the pathway is linked specifically with the visual transduction machinery in the secondary neurons of the retina. With the inclusion of this pathway, the findings broaden the understanding of the existing mechanisms showing how ROS-GC1 is able to receive and transduce diverse Ca^{2+} signals into the cell-specific generation of second-messenger cyclic GMP in the retinal neurons.

Visual transduction is a broad biochemical term used to define the steps involved in the transformation of the patterns of light and darkness into the defined images of shape with depth and color intensity in the visual cortex of the brain. The first biochemical process of visual transduction is phototransduction (reviewed in refs *1* and *2*). It occurs in the outer segments of the photoreceptors (PROS).[1] The photon captured by its receptor rhodopsin causes a decline in the level of cyclic GMP. This results in closure of the cyclic GMP-gated cation (CNG) channels, and hyperpolarization of the photoreceptor plasma membrane. Closure of the channels stops Ca^{2+} from entering the cell; however, a continuous operation of Na^+/Ca^{2+}, K^+ exchanger leads to a decrease in the intracellular Ca^{2+} concentration from ∼500 nM in the dark-adapted photoreceptor cell to less than 100 nM. The decrease in the Ca^{2+} level signals the activation of a membrane guanylate cyclase, ROS-GC. An increased level of synthesis of cyclic GMP, concomitant with the inactivation of the phototransduction cascade, leads to the reopening of the CNG channels and thereby restoration of the dark current of the photoreceptors. Thus, the Ca^{2+}-modulated ROS-GC transduction machinery is a pivotal component of the phototransduction process, and two interlocked second messengers, cyclic GMP and Ca^{2+}, are its critical elements.

The ROS-GC transduction machinery is a two-component system: Ca^{2+} sensor protein, termed GCAP, and the core transduction component, the ROS-GC enzyme. The GCAP senses a change in Ca^{2+} concentration and proportionately adjusts the ROS-GC activity. A decrement in the Ca^{2+} concentration causes stimulation of ROS-GC and an increment inhibition. The identity of native ROS-GC has been revealed by its direct purification from bovine PROS (*3*−*6*), the site of phototransduction; by its subsequent sequencing (*6*) and cloning from the bovine retina based on the sequence of its four peptides (*7*); and by its Ca^{2+}-dependent reconstitution where GCAP acts as a Ca^{2+} sensor protein (*8*, *9*). This original form of ROS-GC has been renamed ROS-GC1 [ret-GC1 or GC-E (*10*, *11*)], with the discovery of its second form, ROS-GC2 (*12*) [retGC2 or GC-F (*11*, *13*)]. To date, most of the biochemical work has been focused on ROS-GC1 because direct purification studies from native PROS have resulted in purification of the ROS-GC1 only, suggesting that ROS-GC2 is a minor form in the outer segments.

Reconstitution studies with recombinant ROS-GC1 indicate that its Ca^{2+} sensor component, GCAP, senses change in the free Ca^{2+} concentration through its two forms: GCAP1 and GCAP2 (*8*, *9*, *14*). ROS-GC1 is a modular protein; it

† This study was supported by U.S. Public Health Service Grants EY 10828 and DC 005349 (R.K.S.) and HL 070015 (T.D.) and Intramural Grant AG00925 (V.V.).

* To whom correspondence should be addressed. Phone: (856) 566-6977. Fax: (856) 566-7057. E-mail: sharmark@umdnj.edu.

‡ These authors contributed equally to this work.

[1] Abbreviations: CNG, cyclic nucleotide-gated cation; BMH, bismaleimidohexane; DMS, dimethyl suberimidate; EGTA, ethylene glycol bis(2-aminoethyl ether)-*N*,*N*,*N*′,*N*′-tetraacetic acid; ELISA, enzyme-linked immunosorbent assay; GCAP, guanylate cyclase activating protein; GMP, guanosine monophosphate; IPL, inner plexiform layer; MALDI-MS, matrix-assisted laser desorption ionization mass spectrometry; myr-neurocalcin δ, N-myristoylated form of neurocalcin δ; ONE-GC, olfactory neuroepithelial membrane guanylate cyclase; OPL, outer plexiform layer; PMSF, phenylmethanesulfonyl fluoride; PROS, photoreceptor outer segments; ROS-GC, rod outer segment membrane guanylate cyclase; SDS−PAGE, sodium dodecyl sulfate−polyacrylamide gel electrophoresis; VILIP, visinin-like protein; wt-r, wild-type recombinant.

10.1021/bi035631v CCC: $27.50
Published on Web 02/21/2004

contains defined GCAP1 and GCAP2 modulatory regions in its intracellular segment (*8*, *14*−*16*). In the current phototransduction model (reviewed in ref *2*), GCAPs sense light-dependent Ca^{2+} fluctuations and, in turn, through their defined domains, cause proportionate changes in ROS-GC1 activity. In the DARK phase, Ca^{2+} is bound to GCAP, and the cyclase is in its basal state. During the LIGHT phase, the free Ca^{2+} concentration decreases, and below 100 nM, ROS-GC is fully activated by Ca^{2+}-free GCAP, resulting in recovery of the DARK state. Thus, the GCAP/ROS-GC1 transduction system is intricately linked with all phases of phototransduction.

Until very recently, the Ca^{2+}-modulated ROS-GC1 transduction system had been assumed to be within the exclusive domain of ROS, where it is solely linked with phototransduction. With the recent studies, this view is changing, however. In photoreceptors, outside PROS, the ROS-GC1 transduction machinery is present also in the presynaptic region of the cone pedicles; therein, it is linked with GCAP1 and mimics the features of its linkage with phototransduction (*17*). Again, in photoreceptors, outside PROS, it is present in the outer plexiform layer (OPL) (*18*). In this case, instead of GCAP1, it coexists with its other Ca^{2+} sensor protein, S100β, which, unlike GCAP1, causes Ca^{2+}-dependent stimulation of ROS-GC1 with a $K_{1/2}$ of 1 μM (*18*). Thus, a remarkable feature of ROS-GC1 is that it is a bimodal Ca^{2+} switch. Through GCAP1, it is inhibited, and through S100β, it is stimulated. The GCAP1- and S100β-modulated domains in ROS-GC1 have been mapped; they are separate, reside at the opposite ends of the catalytic module, and independently modulate ROS-GC1 activity (*17*, *18*; reviewed in refs *2* and *19*). Thus, the cell-specific residence of ROS-GC1 with its Ca^{2+} sensor partner defines the Ca^{2+}-dependent inhibitory or stimulatory status of the ROS-GC transduction machinery. The three known partners of ROS-GC1 are two GCAPs and S100β.

This report defines the biochemical, structural, and functional identity of a new (fourth) Ca^{2+} sensor ROS-GC1 modulator in the retinal neurons. The modulator is the N-myristoylated form of neurocalcin δ (myr-neurocalcin δ). It exists in the membranes of the IPL but is not detected in PROS; thus, it appears to be unrelated to the physiology of phototransduction. At the resting state of the cellular Ca^{2+} concentration, between 100 and 200 nM (*20*), it resides in the proximity of ROS-GC1 in the membranes of nonphotoreceptor neurons, and via its own domain, it stimulates ROS-GC1 in a Ca^{2+}-dependent manner with a $K_{1/2}$ of 0.8 μM. Immunohistochemical analysis shows the presence of neurocalcin δ in the amacrine and ganglion cells. Biochemical analyses indicate that neurocalcin δ and ROS-GC1 are copresent in the inner plexiform layer (IPL). The findings provide a new regulatory mechanism of ROS-GC1 transduction, demonstrate that this pathway exists outside photoreceptor cells, and broaden the view of how ROS-GC1 transduction machinery achieves operational versatility and functional specificity for the diverse Ca^{2+} signals originating in different layers of the retinal neurons.

EXPERIMENTAL PROCEDURES

Purification of Retinal Neurocalcin δ. The isolation of the IPL from fresh bovine retinas was carried out according to the established protocol (*21*), where the fraction has been termed "P2". The IPL was washed with buffer containing 0.32 M sucrose, 10 mM Tris-HCl (pH 7.5), and 2 mM EGTA. The 100000*g* pellet represented the IPL membrane fraction. The supernatant (IPL soluble fraction) was used for purification of neurocalcin δ. This involved two steps, purification on a phenyl-Sepharose column followed by the antibody affinity column. For phenyl-Sepharose column chromatography, the fraction was dialyzed overnight against 100 volumes of buffer containing 20 mM Tris-HCl (pH 8.0), 100 mM NaCl, 1 mM PMSF, and 1 mM $MgCl_2$ (buffer A) containing 1 mM $CaCl_2$ at 4 °C and loaded onto the column (typically, 5 mL) equilibrated with the same buffer. Elution was monitored by the absorbance at 280 nm, and 1 mL fractions were collected (Figure 1A). The column was washed with buffer A (typically, 7−10 column volumes) to remove unbound proteins. Elution of bound proteins occurred with buffer A containing 2 mM EGTA (6 column volumes),

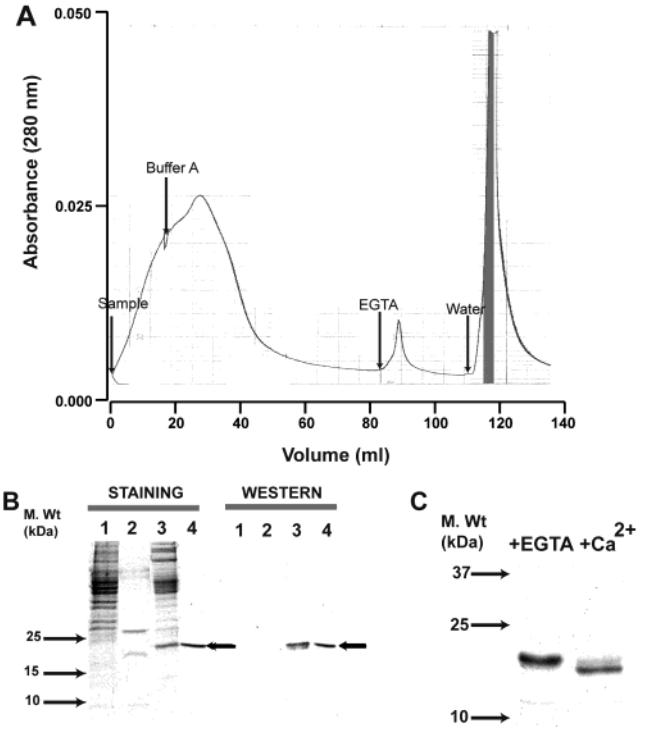

FIGURE 1: Purification of retinal neurocalcin δ. Neurocalcin δ was purified from the retinal IPL soluble fraction via phenyl-Sepharose column chromatography followed by antibody affinity chromatography, as described in Experimental Procedures. The elution profile from the phenyl-Sepharose column is presented in panel A. The absorbance of the eluate was monitored at 280 nm and is plotted as a function of volume. The neurocalcin δ-positive fractions are indicated in the shaded area of the peak. An aliquot of each fraction from both phenyl-Sepharose and antibody affinity columns was analyzed (SDS−15% PAGE) by staining and Western blotting. A representative figure, summarizing the elution profile, is presented in panel B: lane 1, unbound; lane 2, EGTA eluate; lane 3, distilled water eluate; and lane 4, eluate from the antibody affinity column. The left panel (STAINING) presents Coomassie blue staining of the fractions analyzed via SDS−15% PAGE. The right panel (WESTERN) presents the results of probing the same fractions with neurocalcin δ-specific antibody via Western blotting. The band corresponding to neurocalcin δ is denoted with a thick arrow in both panels. Molecular size markers are provided alongside. The Ca^{2+}-dependent shift in the mobility of the purified protein is presented in panel C. The purified neurocalcin δ-immunoreactive protein was analyzed via SDS−15% PAGE. The sample was loaded in the presence of 1 mM Ca^{2+} (+Ca^{2+}) or 1 mM EGTA (+EGTA). Molecular size markers are given alongside.

followed by distilled water (10 column volumes). To identify the fractions containing neurocalcin δ, SDS−15% PAGE analysis was carried out. Fractions were electrophoresed in duplicate. One was used for staining (Coomassie-blue) and the other for Western blot analysis. The neurocalcin δ-immunoreactive protein eluted in the second column volume of distilled water (Figure 1A, gray shaded region of the peak). SDS−PAGE analysis showed this fraction to be a mixture of several proteins, one of which, indicated by the arrow, was revealed to be neurocalcin δ by Western blotting (Figure 1B, lane 3 in STAINING and WESTERN panels). The fractions containing the immunoreactive protein were concentrated and further purified on an antibody affinity column. For generating the antibody affinity column, the neurocalcin δ-specific antibody was purified on a Montage spin column containing ProSep-A media (Millipore) according to the manufacturer's protocol. The purified IgG was coupled to activated Affi-gel Hz matrix (Bio-Rad). The column was extensively washed with 10 mM Tris-HCl (pH 7.5) containing 0.5 M NaCl and equilibrated with buffer B [20 mM Tris-HCl (pH 7.5), 1 mM $MgCl_2$, 0.1 mM $CaCl_2$, and 1 mM PMSF] containing 0.1 M NaCl. The antibody reacting fractions from the phenyl-Sepharose column were pooled and diluted with an equal volume of the same buffer and loaded onto the antibody affinity column. To remove unbound proteins, the column was washed in the following sequence: 20 volumes of buffer B containing 0.1 M NaCl, 5 volumes of buffer B containing 0.5 M NaCl, and, finally, 5 volumes of buffer B containing 0.1 M NaCl. The bound protein was eluted with 0.2 M glycine (pH 2.5). Fractions (1 mL) were collected and neutralized with 0.1 mL of 1 M Tris-HCl (pH 9.0). To detect the fractions containing the antibody reacting protein, SDS−15% PAGE analysis was carried out. Duplicate samples were analyzed by staining (Coomassie blue) and Western blotting. A single protein (~20 kDa) was eluted from the antibody column (Figure 1B, lane 4 in the STAINING panel, denoted with an arrow). This protein also reacted with the neurocalcin δ antibody on Western blot analysis (Figure 1B, lane 4 in the WESTERN panel, denoted with an arrow).

Protein Identification. The purified protein was electrophoresed on an SDS−15% polyacrylamide gel. The gel was stained with Coomassie blue and destained. The gel piece containing the stained protein was excised and used for protein identification. It was subjected to proteolytic digestion with trypsin, and the resultant peptides were analyzed by matrix-assisted laser desorption ionization mass spectrometry (MALDI-MS). Bradykinin and ACTH were used for internal calibration. The masses were used to search the protein database using two independent programs: ProFound and Mascot (Howard Hughes Medical Institute biopolymer laboratory and W. M. Keck Foundation biotechnology resource laboratory at Yale University, New Haven, CT). The purified protein was identified as neurocalcin δ.

Cloning, Expression, and Purification of Recombinant Neurocalcin δ. To clone the cDNA encoding the retinal neurocalcin δ, primers were designed on the basis of the known bovine brain neurocalcin δ sequence: 5′CAGTCCATGGGAAAACAGAACAGCAAGCTGCG-CCCGGA3′ and 5′TGCAAGCTTACGACAGAGAAGCT-GAATTCGAA3′, with introduced *Nco*I and *Hin*dIII (underlined) in the forward and reverse primers, respectively, to facilitate cloning. The amplicon encompassing the entire neurocalcin δ coding region was obtained from the retinal RNA after RT-PCR. It was cloned into the pET21d expression vector and was sequenced to confirm its identity. For protein expression, *Escherichia coli* strain BL21 Codon Plus was transformed with the construct. The bacterial cells were grown in LB medium at 37 °C and induced with 1 mM IPTG when the A_{600} reached 0.6. The cells were harvested 3 h after induction, suspended in buffer A containing 0.1 M NaCl, and frozen at −80 °C until they were used. To obtain the N-myristoylated form, neurocalcin δ and *N*-myristoyltransferase of *Saccharomyces cerevisiae* were coexpressed. BL21 Codon Plus cells were cotransformed with the plasmid pBB131 harboring the *N*-myristoyltransferase and the neurocalcin δ expression vector. Myristic acid was added to the culture at a concentration of 50 μg/mL, 30 min prior to induction with IPTG. Recombinant myr-neurocalcin δ or its nonmyristoylated form was purified from the bacterial lysate by hydrophobic interaction chromatography on phenyl-Sepharose in the presence of 1 mM Ca^{2+}, followed by Q-Sepharose as described previously (*22*).

Antibodies. Characterization of highly specific antibodies raised in rabbit against ROS-GC1 and neurocalcin δ has been described previously (*23*−*25*). The antibodies were enriched by precipitating the immunoglobulin fraction using ammonium sulfate. ELISA and Western blots were used to determine the titer of the enriched antibodies.

Expression Studies. COS-7 cells (simian virus 40-transformed African green monkey kidney cells), maintained in Dulbecco's-modified Eagle's medium with penicillin, streptomycin, and 10% fetal bovine serum, were transfected with the wild-type recombinant (wt-r) ROS-GC1 expression construct by the calcium phosphate coprecipitation technique (*26*). Sixty hours after transfection, cells were washed twice with 50 mM Tris-HCl (pH 7.5) and 10 mM buffer, scraped into 2 mL of cold buffer, homogenized, centrifuged for 15 min at 5000*g*, and washed several times with the same buffer. The resulting pellet represented crude membranes.

Guanylate Cyclase Activity Assay. Membrane fractions were assayed for guanylate cyclase activity as described previously (*27*). Briefly, membranes were preincubated on an ice bath with or without regulatory proteins in the assay system containing 10 mM theophylline, 15 mM phosphocreatine, 20 μg of creatine kinase, and 50 mM Tris-HCl (pH 7.5) adjusted to the appropriate free Ca^{2+} concentrations with precalibrated Ca^{2+}/EGTA solutions (Molecular Probes). The total assay volume was 25 μL. The reaction was initiated by addition of the substrate solution containing 4 mM $MgCl_2$ and 1 mM GTP and maintained by incubation at 37 °C for 10 min. The reaction was terminated by addition of 225 μL of 50 mM sodium acetate buffer (pH 6.2) followed by heating in a boiling water bath for 3 min. The amount of cyclic GMP formed was determined with a radioimmunoassay (*28*).

Western Blot. Western blotting was carried out according to the previously published protocols (*23*−*25*). Briefly, the protein samples were transferred onto nitrocellulose membranes after electrophoresis. The membranes were incubated in Tris-buffered saline containing 0.05% Tween 20 (TBS-T) and 3% bovine serum albumin (BSA) for 1 h at room temperature followed by 1 h incubation in the same solution containing the primary antibody. After the membranes had been washed with TBS-T, incubation was continued for the

same period of time in TBS-T containing 3% BSA and the secondary antibody. After they had been washed in TBS-T, visualization of the immunoreactive protein bands was carried out according to the manufacturer's (Pierce Biotechnology) protocol.

Cross-Linking. Cross-linking was carried out with BMH (bismaleimidohexane), a homobifunctional, sulfhydryl-reactive cross-linker. Membranes were first reduced by addition of 1 mM DTT. Following incubation on ice for 10 min, the membranes were extensively washed with 10 mM HEPES-KOH (pH 7.0), to remove DTT. Cross-linking was carried out in a reaction volume of 40 μL. For the native system, IPL membranes (100 μg of protein equivalent) in 10 mM HEPES-KOH (pH 7.0) and 1 mM $CaCl_2$ were incubated with 10 mM BMH for 60 min at room temperature with shaking. For the reconstituted system, membranes isolated from COS cells expressing ROS-GC1 (100 μg of protein equivalent) were incubated with 2 μg of bacterially expressed and purified recombinant myr-neurocalcin δ under identical conditions. The reaction was stopped by the addition of 4 μL of 1 M Tris-HCl (pH 7.0). Samples were boiled in 6$\times$ sample buffer without DTT, separated on SDS−PAGE (10 or 7%), and transferred to nitrocellulose. Duplicate samples were probed independently with highly specific antibodies against ROS-GC1 or neurocalcin δ. Western blotting was carried out as described previously (*23*, *25*).

Immunohistochemistry. Cryosections of the retina were prepared and used according to the procedure described previously (*17*). Briefly, the retina was fixed for 1 h in 4% formaldehyde at 4 °C; it was cryoprotected in 25% sucrose overnight at 4 °C and sectioned at a thickness of 16 μm (Leica cryostat). To block nonspecific protein binding, sections were incubated in 0.1 M phosphate buffer containing 10% normal goat serum, 5% sucrose, and 0.5% Triton X-100 for 60 min at room temperature. The sections were then incubated in the same solution containing primary antibodies overnight at 4 °C, washed, and incubated in secondary antibodies conjugated to a fluorescent dye and diluted in the blocking solution. Washes were carried out at room temperature (three times, 10 min each) with 0.1 M phosphate buffer containing 5% sucrose. Specimens were mounted using Vectashield mounting medium. Images were acquired using a confocal microscope (Leica). Digital images were processed using commercially available software (ImagePro Plus; Phase3 Imaging Systems and Adobe Photoshop). Controls included immunostaining reactions carried out under identical conditions except that either excess antigen was included or primary antibody was omitted or was replaced with preimmune serum. Staining was insignificant under all these conditions.

Ca^{2+}−Myristoyl Switch. To assess the function of the Ca^{2+}−myristoyl switch, Ca^{2+}-dependent binding of myr-neurocalcin δ to membranes was assayed. In the native IPL membranes, isolation was carried out in the absence or presence of 1 mM Ca^{2+} (Ca^{2+}-enriched condition) or 1 mM EGTA (Ca^{2+}-depleted condition). The membranes were subjected to SDS−15% PAGE, transferred onto a nitrocellulose membrane, and probed with the anti-neurocalcin δ antibody as described previously.

In the *in vitro* assay system, COS membranes transfected with ROS-GC1 were reconstituted with bacterially expressed recombinant myr-neurocalcin δ. The membranes were washed twice with 20 mM Tris-HCl (pH 8.0), 0.1 M NaCl, and 1 mM PMSF (buffer C) and resuspended in the same buffer. Association studies were carried out in a total volume of 25 μL in buffer C. Eight micrograms of recombinant myr-neurocalcin δ was incubated with the membrane (equivalent to 15 μg of protein) in the presence of either 1 mM EGTA or 1 mM EGTA and 2 mM $CaCl_2$ at 22 °C for 20 min. This was followed by centrifugation at 14 000 rpm for 15 min. The pellet was resuspended in 25 μL of buffer C. Both the pellet and the supernatant were subjected to SDS−15% PAGE, and the proteins were transferred onto a nitrocellulose membrane and probed with the anti-neurocalcin δ antibody as described previously.

For dissociation studies, 15 μg of COS membranes transfected with ROS-GC1 incubated with 8 μg of myr-neurocalcin δ in the presence of Ca^{2+} was washed twice with 25 μL of buffer C containing 2 mM EGTA. After the final wash, the pellet was resuspended in 25 μL of buffer C. All the fractions were electrophoresed via SDS−15% PAGE, transferred to nitrocellulose, and probed with the anti-neurocalcin δ antibody.

Surface Plasmon Resonance (SPR) Measurements. Real-time binding analyses were performed at 25 °C, using the BIAcore X system. myr-Neurocalcin δ [150 ng/μL in 50 mM sodium acetate (pH 4.0)] was covalently immobilized on the CM5 sensor chip via the primary amino group using the manufacturer's amine coupling procedure. The amount of immobilized myr-neurocalcin δ was ~0.4 ng/mm^2. The buffer for the mobile phase of the interaction experiments contained 10 mM Tris-HCl (pH 7.5), 150 mM NaCl, 2 mM $CaCl_2$, and 0.005% Surfactant P20. An independent flow cell on the same sensor was subjected to a "blank immobilization" (no neurocalcin δ was added in the preparation of the chip) and used as a control flow cell. The purified ROS-GC1 domain containing amino acids 733−1054 [stock solution at 0.5 μg/μL (10 μM) in the mobile phase buffer] was diluted to varying concentrations (from 0 to 5 μM) in the same buffer and injected into the flow cell. The flow rate was maintained at 10 μL/min. Binding was observed as an increase in resonance units (RU). Specific binding was obtained by subtraction of binding at the control flow cell (no immobilized neurocalcin δ) from that at the experimental cell (neurocalcin δ-coated). The sensor surface was regenerated after each cycle by injection of 5 μL of 0.05 M glycine-HCl (pH 2.5) at a flow rate of 5 μL/min. The binding parameters (k_{on}, k_{off}, K_A, and K_D) for the interaction of the ROS-GC1 domain with immobilized neurocalcin δ were calculated using BiaEvaluation version 3.2. The curves were fitted according to a simple 1:1 interaction with mass transfer. Identical conditions were used to assess binding of S100β and myr-neurocalcin δ to bacterially expressed and purified ROS-GC1 amino acids 963−1054 except that the ROS-GC1 fragment was immobilized by amine coupling and S100β or myr-neurocalcin δ (at 1 μM) was in the mobile phase at a saturating Ca^{2+} concentration of 2 mM.

RESULTS

Characterization of Neurocalcin δ from the Retinal Inner Plexiform Layer

Purification. SDS−PAGE and Western blot analyses using the neurocalcin δ-specific antibody showed that the protein

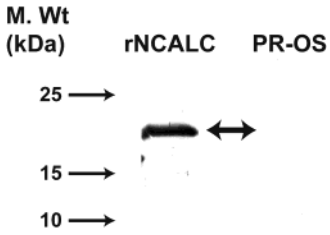

FIGURE 2: Neurocalcin δ is not present in photoreceptor outer segments, as determined by Western analysis. The biochemical fraction corresponding to photoreceptor outer segments (PR-OS) was isolated according to standard protocols. One hundred micrograms of protein was electrophoresed, transferred to nitrocellulose membranes, and probed with the neurocalcin δ-specific antibody. One microgram of recombinant neurocalcin δ (rNCALC) served as a positive control. The position of the immunoreactive band is denoted with a double-headed arrow. Molecular size markers are provided alongside.

isolated from the IPL of the bovine retina was pure (Figure 1B). It migrated as a 20 kDa protein on SDS−15% PAGE in the presence of Ca^{2+}. Addition of EGTA to the protein sample created a gel shift in its migration to 23 kDa (Figure 1C), which is a typical characteristic of the Ca^{2+}-binding proteins (*29*−*31*). Thus, the IPL protein is, or is very similar, to the Ca^{2+}-binding protein neurocalcin δ.

Microsequencing. The tryptic digest of the IPL protein yielded 52 peptides. The mass spectral analysis of these peptides demonstrated that the masses were identical to those generated from neurocalcin δ derived from a variety of mammalian brain sources, including bovine and the human forms (*32*, *33*). Because the N-terminus was modified, N-terminal sequencing was not successful. Mass spectral analysis showed that the major modification at the N-terminus is N-myristoylation. Therefore, the IPL 20 kDa protein is neurocalcin δ, and it exists in its major N-acylated form as myristoylated.

Molecular Cloning of Retinal Neurocalcin δ. The sequences of all the tryptic peptides of the native IPL protein, neurocalcin δ, were encoded in the full-length cDNA clone, indicating that the mRNA encoding the protein had been cloned. The cDNA-based sequence of the protein was identical to the published sequence of bovine brain neurocalcin δ (*32*). The protein contains four Ca^{2+}-binding EF-hand motifs, yet only three (EF2, EF3, and EF4) are predicted to be functional (*32*, *34*, *35*). Thus, the IPL neurocalcin δ is identified at a molecular and chemical level.

Neurocalcin δ Is Undetectable in the Photoreceptor Outer Segments. To assess the possible involvement of neurocalcin δ in any of the Ca^{2+}-modulated processes operating in the PROS, the outer segments were surveyed for their content of neurocalcin δ. No immunoreactivity was observed with the neurocalcin δ antibody [Figure 2, lane PR-OS; recombinant neurocalcin δ (rNCALC) served as a positive control], indicating that neurocalcin δ has no role in the phototransduction process. This conclusion is further supported by the immunohistochemical studies provided below.

Some Amacrine and Ganglion Cells of the Retina Express Neurocalcin δ. To determine the cell-specific expression of neurocalcin δ in the retinal neurons, cryosections of the bovine retina were probed with the neurocalcin δ-specific antibody (Figure 3A). Strong staining was observed in a significant number of amacrine cells (some denoted with white arrows), in large ganglion cells (one is denoted with a colored arrow), and in the distinct regions of the IPL. The outer segments (OS) exhibited only insignificant staining. Minor staining was also observed in the inner segments, particularly those of the cones, and in the perinuclear layer of defined cells in the outer nuclear layer (ONL). There was no staining in the bipolar cells.

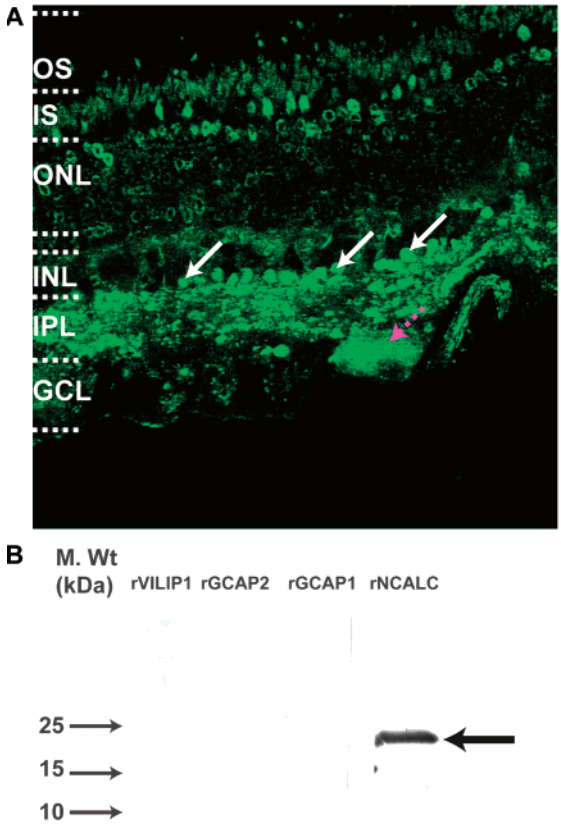

FIGURE 3: Neurocalcin δ is expressed in the amacrine and ganglion cells of the retina. (A) Immunohistochemical analysis. Cryosections of bovine retina were immunostained for neurocalcin δ. Abbreviations: OS, outer segments; IS, inner segments; ONL, outer nuclear layer; OPL, outer plexiform layer; INL, inner nuclear layer; IPL, inner plexiform layer; GCL, ganglion cell layer. Neurocalcin δ staining (green) is strong in the IPL, amacrine cells (INL layer; some are denoted with white arrows), and some ganglion cells (GCL layer; one is denoted with a pink arrow). Some staining of the cone inner segments is also seen. (B) Specificity of the neurocalcin δ antibody. One microgram each of recombinant VILIP1 (rVILIP1), GCAP1 (rGCAP1), GCAP2 (rGCAP2), and neurocalcin (rNCALC) were electrophoresed and subjected to Western analyses. The immunoreactive band is denoted with a thick arrow. Molecular size markers are provided alongside.

These results support the conclusion that neurocalcin δ is not present in the outer segment of the photoreceptors. They also suggest that neurocalcin δ is also absent in the bipolar cells. Its primary presence is in certain amacrine and ganglion neurons and in some structures located in the distinct regions of the IPL. It is noteworthy that the neurocalcin δ antibody used in this study is exclusively specific to neurocalcin δ and has no cross-reactivity with any of its homologous neuronal Ca^{2+} sensor proteins (reviewed in refs *36* and *37*): VILIP1, GCAP1, and GCAP2 (Figure 3B). The expression of neurocalcin δ in the amacrine and ganglion cells has been reported previously (*38*). Due to the lack of antibody specificity among the multiple "isoproteins" of neurocalcin δ, Nakano *et al.* (*38*), however, were unable to differentiate between these isoproteins.

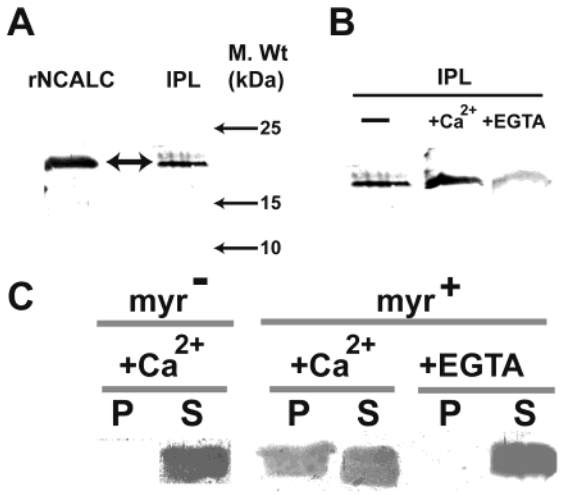

FIGURE 4: Neurocalcin δ is expressed in the IPL membrane fraction and exhibits Ca^{2+}-dependent association. (A) Presence in the IPL membrane. The inner plexiform layer (IPL) fraction was isolated from retina, electrophoresed, and analyzed by Western blotting as described in Experimental Procedures. Fifty micrograms of the membrane protein was loaded. One microgram of bacterially expressed and purified recombinant myr-neurocalcin δ (rNCALC) served as a positive control. The highly specific neurocalcin δ antibody was used as the probe. The immunoreactive band is denoted with a double-headed arrow. Molecular size markers are given alongside. (B) Ca^{2+}-dependent association in the native system. Western analysis was carried out with IPL membrane fractions from retina isolated in the presence of 1 mM Ca^{2+} (+Ca^{2+}) or 1 mM EGTA (+EGTA) or in the absence of either additive (−). Fifty micrograms of protein was loaded in each lane. (C) Ca^{2+}-dependent association in the reconstituted system. Bacterially expressed and purified recombinant retinal neurocalcin δ was incubated with membranes from COS cells expressing recombinant ROS-GC1 in the presence of Ca^{2+} (+Ca^{2+}) or EGTA (+EGTA). The neurocalcin δ was in its myristoylated form (myr^+) or nonmyristoylated form (myr^-). Incubation, subsequent isolation of the pellet (P) and supernatant (S) fractions, and analysis by Western blotting were carried out as described in Experimental Procedures.

Membrane Portion of the IPL Contains the myr-Neurocalcin δ. To act as a Ca^{2+} sensor protein involved in the membrane signaling processes, neurocalcin δ must be able to readily associate with the membrane fraction. This was assessed by the Western blot analysis of the native IPL. The native membrane fraction was isolated and probed with the neurocalcin δ-specific antibody. A single immunoreactive band (denoted with a double-headed arrow) was observed (Figure 4A, IPL). The mobility of the immunoreactive protein was identical to that of the recombinant myr-neurocalcin δ (in Figure 4A, compare IPL and rNCALC). Therefore, neurocalcin δ is present in the IPL membrane fraction.

The presence of myr-neurocalcin δ in the IPL membranes has important bearing on its being a receiver and transmitter of Ca^{2+} signal transduction processes. Extensive studies on the role of the myristoyl group in neuronal calcium sensor proteins, particularly recoverin and the bovine brain neurocalcin δ, have revealed the following: (i) in the Ca^{2+}-free state, the myristoyl group is tethered inside a hydrophobic pocket by the three EF-hands; (ii) upon binding Ca^{2+} by the EF-hands, it is extruded from the pocket; and (iii) the exposed myristoyl group promotes binding to membranes and/or protein targets (*31*, *39*−*45*). The biochemical term for this process is the "Ca^{2+}−myristoyl switch". Because the IPL neurocalcin δ is myristoylated, it was possible that, like recoverin, it has a functional Ca^{2+}−myristoyl switch.

This prediction was investigated in greater detail. Both the native IPL and the heterologous reconstituted systems were used for this purpose, and in both systems, similar results were obtained. In the native system, the IPL membranes were isolated under three Ca^{2+} conditions: (1) no treatment, (2) Ca^{2+}-treated (1 mM Ca^{2+}), and (3) Ca^{2+}-depleted (washed with 1 mM EGTA). The fractions were analyzed by Western blotting, using the neurocalcin δ antibody probe. The results are presented in Figure 4B. A single immunoreactive band, corresponding to neurocalcin δ, was seen in all three fractions. The intensity of the bands was different, however. The most intense band was in the Ca^{2+}-treated fraction (Figure 4B, lane +Ca^{2+}), which was followed by the fraction without treatment (Figure 4B, lane −) and then by the Ca^{2+}-depleted fraction (Figure 4B, lane +EGTA). These results demonstrate that (i) Ca^{2+} enhances the membrane anchoring property of neurocalcin δ, (ii) there is a sufficient concentration of residual Ca^{2+} in the IPL to keep neurocalcin δ membrane-bound, and (iii) it is difficult to remove this residual amount of Ca^{2+} from the native membranes. Thus, some neurocalcin δ is always membrane-bound, and is ready to initiate Ca^{2+} signal transduction processes occurring within millisecond time intervals, a feature that is essential for the transmission of visual signals.

In the heterologous system, the nonmyristoylated and myristoylated forms of neurocalcin δ were incubated with the membranes of COS cells in the presence (1 mM Ca^{2+}) or absence of Ca^{2+} (1 mM EGTA) and the membranes were probed for the presence of neurocalcin δ by Western blot analysis. Membranes incubated with 1 mM Ca^{2+} showed an intense neurocalcin δ band when incubated with myr-neurocalcin δ (Figure 4C, panel myr^+, lane P under +Ca^{2+}). In contrast, no band was observed with the nonmyristoylated form of neurocalcin δ in the presence of Ca^{2+} (Figure 4C, panel myr^-, lane P) or in the Ca^{2+}-depleted membranes (Figure 4C, panel myr^+, lane P under +EGTA). These results again show that the myristoyl group of neurocalcin δ is critical in making the neurocalcin δ membrane-bound, and when the group is missing, neurocalcin δ is no longer membrane-bound. Thus, in the IPL, neurocalcin δ contains an active Ca^{2+}−myristoyl switch and a fraction of neurocalcin δ is always membrane-bound.

These studies establish that the functional form of neurocalcin δ in the IPL is the myristoylated form and that, under native conditions, the IPL membranes contain a sufficient concentration of Ca^{2+} to keep neurocalcin δ membrane-bound, ever ready to receive and transmit the Ca^{2+} signals in quick succession.

Characterization of the Neurocalcin δ-Modulated Ca^{2+} Signaling Pathway in the IPL

The IPL Fraction of the Retina Contains a Membrane Guanylate Cyclase, which Exhibits a Biphasic Manner of Ca^{2+} Modulation. The PROS and the OPL components of the photoreceptors contain two distinct Ca^{2+}-modulated membrane guanylate cyclase (ROS-GC1) transduction pathways. In PROS, the pathway is linked with phototransduction, and the Ca^{2+} sensor component of ROS-GC1 is GCAP.

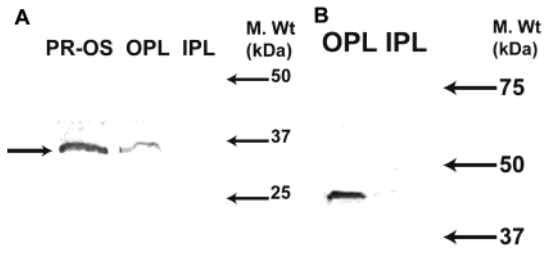

FIGURE 5: Purity of the IPL fraction. Photoreceptor outer segment (PR-OS), outer plexiform layer (OPL), and inner plexiform layer (IPL) fractions were isolated from retina, electrophoresed, and analyzed by Western blotting as described in Experimental Procedures. Fifty micrograms of membrane protein was loaded in each lane. (A) PR-OS, OPL, and IPL fractions were probed with an antibody against rhodopsin. (B) OPL and IPL fractions were probed with a cone arrestin antibody. Molecular size markers are given alongside.

GCAP senses the Ca^{2+} impulses and inhibits the cyclase (reviewed in refs *2* and *19*). In the OPL, Ca^{2+} operates through two reciprocal pathways. One pathway is specific to the cone pedicles (*17*). Like PROS, in the pedicles, the Ca^{2+} sensor component of ROS-GC1 is GCAP1 and the Ca^{2+} impulses inhibit the cyclase; in the other OPL region, the Ca^{2+} sensor component is S100β and the Ca^{2+} impulses stimulate ROS-GC1 (*17*, *18*). To ensure that these cell-specific pathways do not interfere with the IPL results, it was made certain that the IPL fraction was not contaminated with PROS or OPL. Two probes were used for this purpose: a rhodopsin antibody to test for the presence of rods and a monoclonal antibody against cone pedicles (7G6) for the cones. The Western blot results are presented in panels A and B of Figure 5, respectively. Neither antibody exhibited reactivity with IPL; however, in positive controls, the two antibodies exhibited PROS- and OPL-specific reactivity (Figure 5A, lane PR-OS and OPL; Figure 5B, lane OPL). Thus, the IPL preparation is not contaminated with PROS or OPL and is suitable for exploring the presence of the Ca^{2+}/neurocalcin δ-modulated guanylate cyclase signaling pathway in the IPL.

The native IPL membrane guanylate cyclase responded in a biphasic fashion to the incremental concentrations of Ca^{2+} (Figure 6A): the range from 10 nM to 0.5 μM inhibited the cyclase, and the higher ranges stimulated it. The inhibitory value (IC_{50}) for Ca^{2+} was ~60 nM, and the stimulatory (EC_{50}) was ~1 μM. Thus, the IPL contains a native Ca^{2+}-modulated membrane guanylate cyclase transduction system, which is both stimulated and inhibited by free Ca^{2+} concentrations. Although this investigation was focused on only the identification of the stimulated system, the IC_{50} value of Ca^{2+} suggests that the inhibitory system in IPL is GCAP-modulated.

To assess if the Ca^{2+}-stimulated native IPL membrane guanylate cyclase was neurocalcin δ-modulated, myr-neurocalcin δ was incubated with the IPL membrane fraction and assayed for guanylate cyclase activity. Addition of neurocalcin δ stimulated endogenous membrane guanylate cyclase in a dose-dependent fashion with an EC_{50} of 0.8 μM. The stimulation was ~2.5-fold over the basal value (Figure 6B). When the incubation was carried out with Ca^{2+}-depleted (EGTA-treated) membranes, the maximal stimulation of the cyclase increased to ~4-fold (Figure 6C). These results indicate two things. One, they show that the native IPL

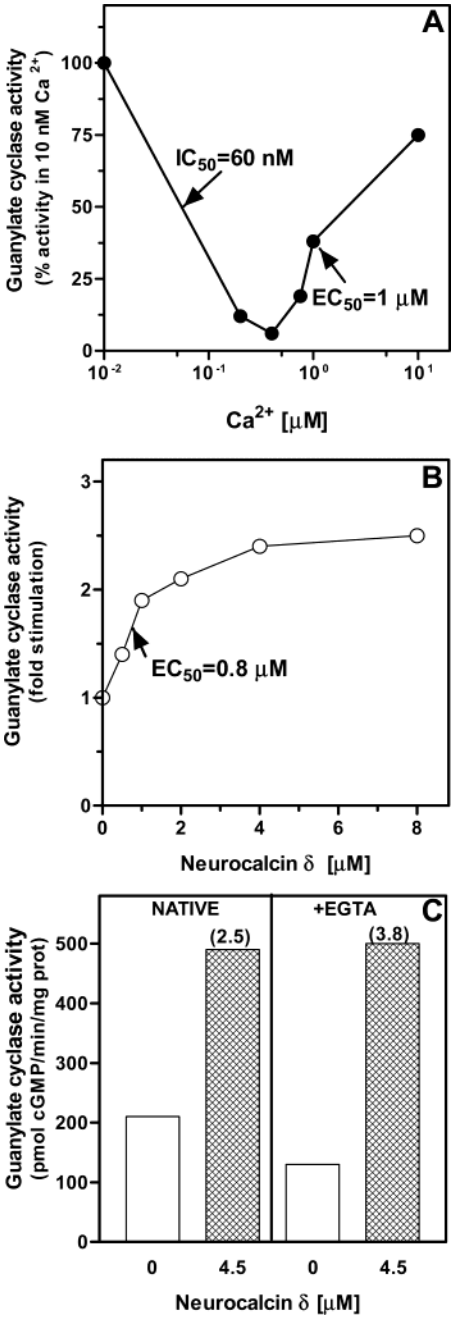

FIGURE 6: Ca^{2+} regulation of guanylate cyclase activity in the IPL. The IPL fraction was isolated from the bovine retina, and the membranes were assayed for guanylate cyclase activity as described in Experimental Procedures. The experiments were carried out in triplicate and repeated three times with separate membrane preparations. The results presented here are from one representative experiment. Error bars are smaller than the symbols. (A) Response to Ca^{2+}. The IPL membranes were incubated in the presence of incremental concentrations of Ca^{2+}. The results are expressed as a percentage of maximal activity. (B) Response to myr-neurocalcin δ. The IPL membranes were incubated in the presence of 1 μM Ca^{2+} and incremental concentrations of myr-neurocalcin δ. The results are expressed as the fold stimulation over basal activity. (C) Response to myr-neurocalcin δ by Ca^{2+}-depleted IPL membranes. IPL membranes isolated in the absence (NATIVE) or presence of 1 mM EGTA (+EGTA) were assayed for guanylate cyclase activity in the presence of 1 μM Ca^{2+} and the indicated concentration of myristoylated neurocalcin δ. The activity is expressed as picomoles of cyclic GMP synthesized per minute per milligram of protein. The fold stimulation over basal activity is given in parentheses.

membranes contain a neurocalcin δ-modulated membrane guanylate cyclase transduction system. Two, they show that in its native state the cyclase exists with Ca^{2+}-bound myr-neurocalcin δ and, as a consequence, is partially active. This interpretation rationalizes the previous finding, which showed the presence of Ca^{2+}-dependent membrane-bound myr-neurocalcin δ in the native IPL membranes.

The Membrane Guanylate Cyclase, ROS-GC1, Is Linked with the Neurocalcin δ-Modulated Ca^{2+} Signaling in the IPL. Reconstitution studies in the heterologous system of COS cells have shown that the recombinant neurocalcin δ stimulates ROS-GC1 in a Ca^{2+}-dependent fashion (*46*). To determine if the Ca^{2+}-dependent myr-neurocalcin δ-stimulated native IPL cyclase is ROS-GC1, the IPL membrane cyclase was subjected to four independent verifications.

(1) Verification 1: Biochemical Identity. ROS-GC1 is the original member of the Ca^{2+}-modulated membrane guanylate cyclase subfamily whose identity was established first in the ROS region of the retina (*7*). Subsequently, immunohistochemical studies with antibodies against retinal guanylate cyclase have also localized the cyclase to ROS; however, these antibodies did not distinguish between the ROS-GC forms (*47*, *48*). To make a biochemical comparison between the native forms of the IPL membrane guanylate cyclase and ROS-GC1 present in the outer segments and retina, Western blot analysis of these fractions was carried out with a ROS-GC1-specific antibody according to the previous protocol (*23*). A single 118 kDa immunoreactive band was detected in all three fractions (Figure 7A), indicating that the native IPL membrane guanylate cyclase is biochemically indistinguishable from the ROS-GC1 present in the PROS region of the retina. It is important to note that the ROS-GC1 antibody used in this study does not cross-react with the two other remaining ROS-GC1 subfamily members: ROS-GC2 and ONE-GC (*24*, *25*).

(2) Verification 2: Functional Identity. ROS-GC1 is a bimodal Ca^{2+} switch (reviewed in refs *2* and *19*). Its two distinctive functional features are that the Ca^{2+} signal inhibits it when it is present with a GCAP and the signal stimulates it with S100β (reviewed in ref *19*). Ca^{2+}-free GCAP1 stimulated the native IPL membrane guanylate cyclase in a dose-dependent fashion with an EC_{50} of 1 μM (Figure 7B), and Ca^{2+}-saturated S100β stimulated the cyclase in a dose-dependent fashion with an EC_{50} of 1 μM (Figure 7C). Both these EC_{50} values are comparable with the established values for the wt-r and native ROS-GC1 (*8*, *49*−*51*). Thus, ROS-GC1 is present in the native IPL membrane.

(3) Verification 3: Physical Interaction. To have functional relevance at the physiological level, neurocalcin δ and ROS-GC1 must reside in proximity of each other. This parameter in the native IPL was determined by cross-linking studies. The homobifunctional, sulfhydryl-reactive BMH was used as a cross-linker. In the absence of the cross-linker, the ROS-GC1 and neurocalcin δ antibodies identified only the respective monomers (Figure 8A, − lanes). With the cross-linker, both neurocalcin δ and ROS-GC1 antibodies identified a common immunoreactive band at ~280 kDa (Figure 8A, + lanes, denoted with a double-headed arrow). The size is that expected for a ROS-GC1 dimer−neurocalcin δ dimer complex. Previous studies have shown that the functional unit of ROS-GC1 is a dimer (*52*−*55*). It has also been shown that bovine neurocalcin δ exists as a dimer in

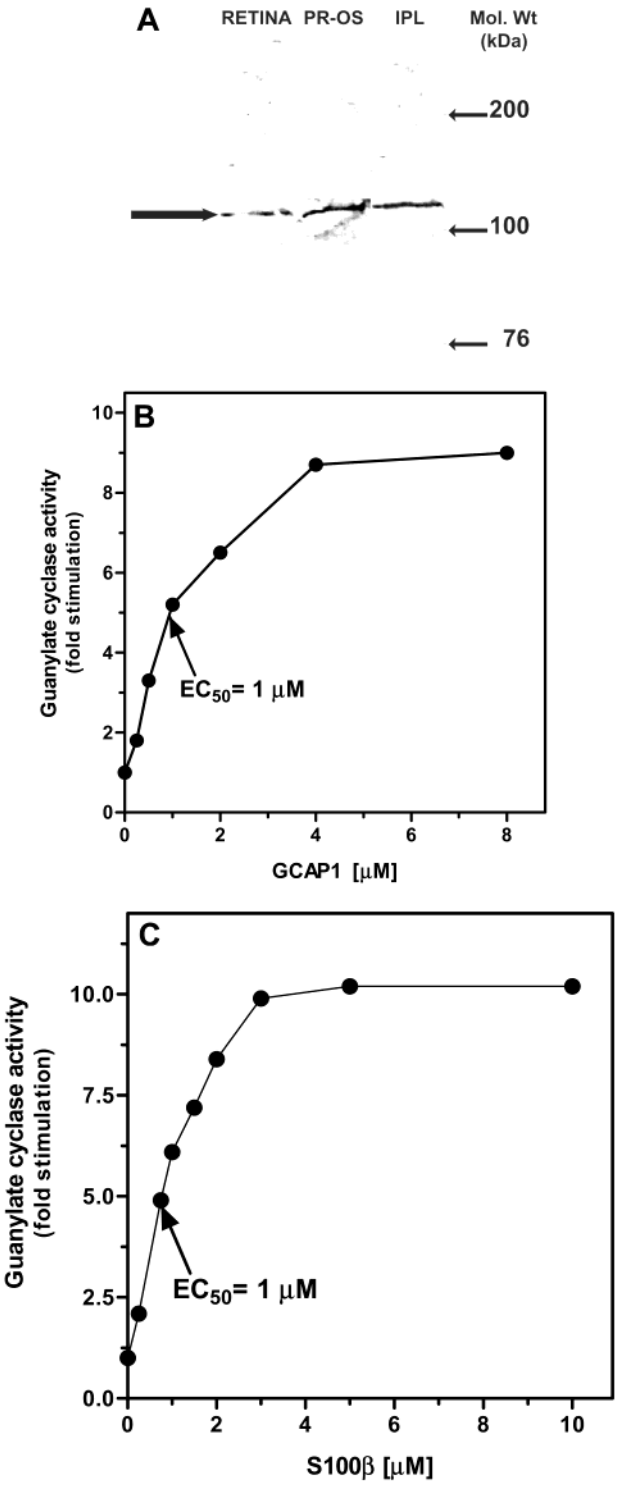

FIGURE 7: Ca^{2+}/neurocalcin δ-regulated membrane guanylate cyclase in the IPL is ROS-GC1. Membrane fractions from whole retina (RETINA), photoreceptor outer segments (PR-OS), and the inner plexiform layer (IPL) were isolated as described in Experimental Procedures. (A) Western analysis with membrane fractions from whole retina (RETINA), photoreceptor outer segments (PR-OS), and the IPL fraction (IPL) was performed with the ROS-GC1 antibody (100 μg of protein/lane). Molecular size markers are given alongside. The position of the immunoreactive band is denoted with a thick arrow. (B and C) Membranes of the IPL fraction were assayed for guanylate cyclase activity in the presence of incremental concentrations of (B) GCAP1 at 10 nM Ca^{2+} or (C) S100β at 10 μM Ca^{2+}. The experiments were carried out in triplicate and repeated three times with separate membrane preparations. The results are from one representative experiment.

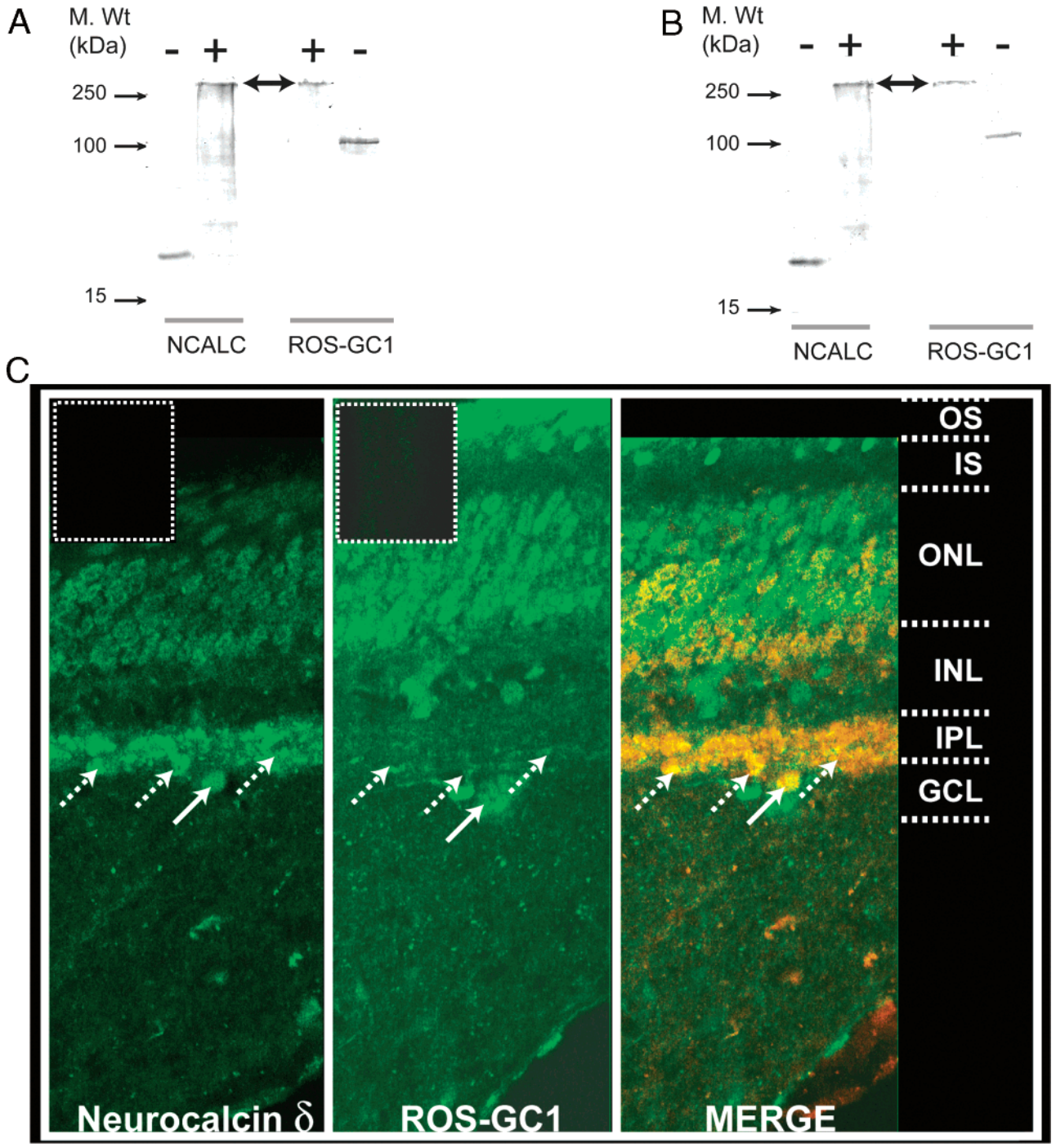

FIGURE 8: ROS-GC1 and neurocalcin δ are in physical proximity in the IPL. Cross-linking and immunohistochemical analyses. Cross-linking was carried out as described in Experimental Procedures. Duplicate samples were electrophoresed on SDS−PAGE gels and probed by Western blotting with the ROS-GC1 or neurocalcin δ antibody. The results are presented in the respective panels. The equivalent of 50 μg of membrane protein was loaded in each lane. A common band, corresponding to ~280 kDa, is observed with both antibodies in the presence of the cross-linker (+ lanes) and is denoted with an arrow. Only the monomer (neurocalcin δ or ROS-GC1) is observed in the absence of the cross-linker (− lanes). Molecular size markers are given alongside. (A) In the native system, IPL membranes were isolated and incubated in the presence or absence of added cross-linker BMH. (B) In the reconstituted system, membranes (50 μg of protein equivalent) isolated from COS cells expressing ROS-GC1 were incubated with bacterially expressed and purified myr-neurocalcin δ (1 μg). (C) For immunohistochemical analyses, consecutive cryosections of bovine retina were analyzed as described in Experimental Procedures. Abbreviations: OS, outer segments; IS, inner segments; ONL, outer nuclear layer; OPL, outer plexiform layer; INL, inner nuclear layer; IPL, inner plexiform layer; GCL, ganglion cell layer. Staining with the neurocalcin δ and ROS-GC1 antibodies is presented in their respective panels. Neurocalcin δ staining (green) is strong in the IPL, amacrine cells (not seen in the field), and some ganglion cells (GCL layer; one is denoted with an arrow). Some staining of the cone inner segments is also seen. No staining was observed when the reaction was carried out in the presence of a 50-fold excess of the antigen. The result is presented as an inset. ROS-GC1 staining is observed through multiple retinal layers, with the most intense staining in the outer segments. Staining in the lower strata of IPL and ganglion cell is indicated: IPL, dashed arrow; ganglion cell, solid arrow. All staining was eliminated by the inclusion of a 50-fold excess of antigen (inset). The neurocalcin δ staining was converted to a red/orange color and aligned with the ROS-GC1 staining using ImagePro Plus. The result is presented in the MERGE panel. Regions positive for both ROS-GC1 and neurocalcin δ appear yellow and are observed in the lower strata of the IPL (some denoted with dashed arrows) and ganglion cells (one in the field denoted with an arrow).

solution (*31*). The size of the cross-linked complex is consistent with a ROS-GC1 dimer binding to a neurocalcin δ dimer. To verify this result, the experiment was repeated with a different cross-linker, DMS. Again, the common ~280 kDa band reacted with both the neurocalcin δ and ROS-GC1 antibodies (data not shown).

To further verify these results obtained with the native IPL system, cross-linking experiments were repeated in a reconstituted, heterologous system: membranes isolated from COS cells expressing ROS-GC1 and bacterially expressed and purified recombinant myr-neurocalcin δ. A common immunoreactive band, ~280 kDa, was observed in only the presence of the cross-linker (Figure 8B, denoted with a double-headed arrow). The band was identical in its mobility to that observed in the native IPL membrane.

It is noteworthy that additional minor bands are observed with the neurocalcin δ antibody probe in the presence of the cross-linker (Figure 8A, + lane, NCALC panel), indicating that this protein may interact with several proteins other than ROS-GC1 in the IPL.

(4) Verification 4: Colocalization. To investigate if ROS-GC1 and neurocalcin δ, in addition to being proximal, also colocalize in the same cellular compartments, immunohistochemical analyses were carried out. Because both antibodies are raised in rabbits, for colocalization experiments, consecutive cryosections were independently stained with antibodies against ROS-GC1 or neurocalcin δ; identical regions were then chosen, on the basis of markers such as blood vessels, for analyses to determine colocalization. One such region is presented in Figure 8C. Individual staining with the neurocalcin δ and ROS-GC1 antibodies of identical regions from retinal sections are presented in their respective panels. Staining is in green. Distinct patterns of staining are observed with the two antibodies. Positive staining with neurocalcin δ is primarily in the inner retina: defined regions distributed throughout the multiple strata of the IPL (some denoted with dashed arrows in Figure 8C, NEUROCALCIN δ) and ganglion cells (one in the field denoted with an arrow in Figure 8C, NEUROCALCIN δ) are stained. No staining was observed when the reaction was carried out in the presence of a 50-fold excess of the antigen (Figure 8C, NEUROCALCIN δ, inset). Positive staining with the ROS-GC1 antibody is spread throughout the retinal layers, consistent with previous findings (*17*, *18*, *47*, *48*). The most intense staining is observed in the layer of outer segments. In addition, staining is observed in the ONL, some cells in the INL, lower strata of the IPL (denoted with dashed arrows in Figure 8C, ROS-GC1), and ganglion cells (one denoted with an arrow in Figure 8C, ROS-GC1). Staining was insignificant in the presence of a 50-fold excess of antigen (Figure 8C, ROS-GC1, inset), demonstrating the specificity of the antibody. After color conversion of neurocalcin δ to red/orange, the neurocalcin and ROS-GC1 panels were merged using ImagePro Plus (Figure 8C, MERGE). Regions that are positive for both neurocalcin δ and ROS-GC1 appear yellow and are observed in the lower strata of the IPL (some denoted with dashed arrows in Figure 8C, MERGE) and ganglion cells (one in the field denoted with an arrow in Figure 8C, MERGE). Thus, neurocalcin δ and ROS-GC1 appear to be colocalized in the lower strata of the IPL and a subpopulation of ganglion cells.

Direct Binding Studies

myr-Neurocalcin δ Binds the Biologically Active ROS-GC1 Domain, Amino Acids 733−1054, in a Ca^{2+}-Dependent Fashion with High Affinity. Reconstitution studies with the deleted and hybrid mutants have suggested that the biologically active neurocalcin δ modulatory site in ROS-GC1 resides within the fragment of amino acids 731−1054 (*46*). The investigation presented here was designed to assess (i) the neurocalcin δ-dependent biological activity of the fragment and (ii) whether the fragment binds neurocalcin δ directly if it is, indeed, biologically active. The fragment was bacterially expressed and purified according to the previously described protocol (*52*). Consistent with the previous results (*52*), it contains inherent guanylate cyclase activity. The activity was 6 pmol of cyclic GMP min^{-1} (mg of protein)$^{-1}$ (Figure 9A, aa733−1054 fragment). Thus, it is biochemically active. When the fragment was incubated with a series of concentrations of the recombinant form of myr-neurocalcin δ in the presence of saturated amounts of Ca^{2+} (10 μM), it showed a concentration-dependent increment in its cyclase activity (Figure 9A). The EC_{50} value for neurocalcin δ was 1.2 μM, and the maximal stimulation of the enzyme was ~2.5-fold over its basal value; for the wild type, it was 5-fold (in Figure 9A, compare wt-rROS-GC1 with aa733−1054 fragment). The results show that the neurocalcin δ-dependent stimulatory profiles of the soluble fragment and the wild-type ROS-GC1 are very similar: compare the EC_{50} of 0.8 μM for the wild type with the value of 1.2 μM for the soluble fragment. Thus, the fragment is biologically active and is appropriate for the direct binding studies with neurocalcin δ.

Direct binding between neurocalcin δ and the ROS-GC fragment was assessed by surface plasmon resonance (SPR) spectroscopy. myr-Neurocalcin δ was immobilized on a sensor chip. The ROS-GC1 fragment was applied in the mobile phase. Real-time binding of the ROS-GC1 fragment with neurocalcin δ was assessed as an increase in resonance units. To determine if Ca^{2+}, essential for neurocalcin δ-mediated regulation of ROS-GC1, is also essential for binding, initial experiments were carried out in the absence or presence of Ca^{2+}. Results presented in Figure 9B clearly demonstrate that no binding is observed in the absence of Ca^{2+} (in the presence of 1 mM EGTA, Figure 9B, +EGTA). Binding of neurocalcin δ with the ROS-GC1 fragment occurs only in the presence of Ca^{2+} (in Figure 9B, compare $+Ca^{2+}$ with +EGTA). These results demonstrate that binding of myr-neurocalcin δ to ROS-GC1 is Ca^{2+}-dependent and direct and that the neurocalcin δ-binding domain in the ROS-GC1 fragment resides between amino acids 733 and 1054.

Further experiments were designed to determine the binding parameters for the ROS-GC1−neurocalcin δ pair. Incremental concentrations of the ROS-GC1 fragment (from 0 to 5 μM) in the mobile phase at the saturated Ca^{2+} concentration of 2 mM resulted in a dose-dependent increase in the level of binding to neurocalcin δ (Figure 9C). The response at equilibrium (R_{eq}) was plotted as a function of the fragment concentration to calculate the half-maximal binding (EC_{50}) of neurocalcin δ with ROS-GC1, which was 0.5 μM (Figure 9D; 8−10 determinations of three independent data sets). This value is comparable to the EC_{50} value of 0.8 μM observed for the neurocalcin δ-dependent stimula-

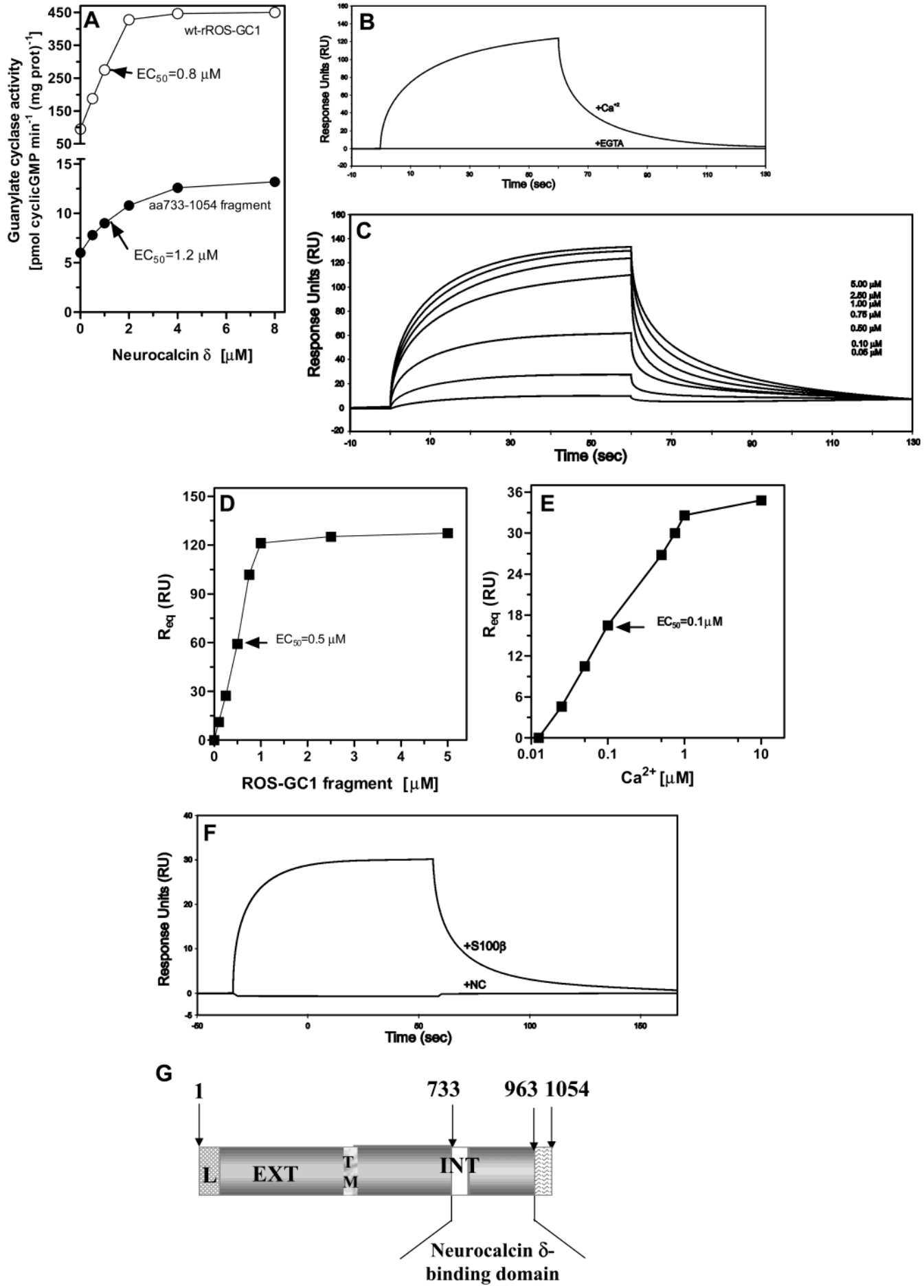
A
wt-rROS-GC1
EC50=0.8 μM
aa733-1054 fragment
EC50=1.2 μM
Guanylate cyclase activity
[pmol cyclicGMP min-1 (mg prot)-1]
Neurocalcin δ [μM]
B
+Ca+2
+EGTA
Response Units (RU)
Time (sec)
C
5.00 μM
2.50 μM
1.00 μM
0.75 μM
0.50 μM
0.10 μM
0.05 μM
Response Units (RU)
Time (sec)
D
EC50=0.5 μM
Req (RU)
ROS-GC1 fragment [μM]
E
EC50=0.1μM
Req (RU)
Ca2+ [μM]
F
+S100β
+NC
Response Units (RU)
Time (sec)
G
1
733
963 1054
L
EXT
TM
INT
Neurocalcin δ-
binding domain

tion of ROS-GC1 (Figure 6B). Other binding parameters were as follows: k_{on} (association rate constant) = 5.4×10^4 M^{-1} s^{-1}, k_{off} (dissociation rate constant) = 2.3×10^{-2} s^{-1}, K_A (equilibrium association constant) = 2.3×10^6 M^{-1}, and K_D (equilibrium dissociation constant) = 4.2×10^{-7} M. These values indicate that the binding is of high affinity, and that the association as well as dissociation rates between neurocalcin δ and the ROS-GC1 fragment are rapid. It is also noted that the calculated K_D value for the neurocalcin δ−ROS-GC1 interaction, 426 nM, is in good agreement with the value of half-maximal binding (EC_{50}) at equilibrium, 500 nM (Figure 9D).

To determine the EC_{50} value of Ca^{2+} needed for binding neurocalcin δ with the ROS-GC1 fragment, real-time binding experiments with incremental concentrations of Ca^{2+} at a constant concentration of the ROS-GC1 domain of 1 μM were conducted. A dose-dependent increase in the level of binding was observed (Figure 9E). A plot of equilibrium binding (R_{eq}) as a function of the Ca^{2+} concentration yielded an EC_{50} value of 0.1 μM for Ca^{2+} (Figure 9E), indicating that the optimum interaction of neurocalcin δ with ROS-GC1 occurs at 100 nM Ca^{2+}. This concentration of Ca^{2+} is within the resting state, 100−200 nM, of a cell (*20*). Results presented earlier (Figure 4) show that under native conditions, the Ca^{2+}−myristoyl switch is active in the IPL and myr-neurocalcin δ is bound to the membranes of the IPL, where ROS-GC1 resides. Results from the direct binding experiments show that ROS-GC1 exists as a complex with Ca^{2+}-bound neurocalcin δ in the IPL membranes even in the resting state of the cell.

The Neurocalcin δ-Binding Domain in ROS-GC1 Is Specific to Itself. Besides housing the neurocalcin δ binding domain, the ROS-GC1 fragment, amino acids 733−1054, also houses the S100β-binding domain (*18*). S100β is another Ca^{2+}-dependent modulator of ROS-GC1 (*18*, *50*, *51*; reviewed in refs *56* and *57*). The S100β-binding domain has recently been mapped (*18*). It is composed of two regulatory sites in ROS-GC1. One site comprises amino acids Gly^{962}−Asn^{891}; the other comprises amino acids Ile^{1030}−Gln^{1041}. To determine if these two sites overlap with the neurocalcin δ-binding site, the fragment of amino acids 963−1054 was bacterially expressed, purified, and immobilized on a BIAcore sensor chip. S100β or myr-neurocalcin δ was applied in the mobile phase. Consistent with the previous results, this fragment bound S100β with an EC_{50} of 395 nM (*18*); however, it did not bind myr-neurocalcin δ (Figure 9F). Thus, the neurocalcin-binding domain in ROS-GC1 is distinct from that of S100β, is specific to itself, and resides in the region between amino acids 732 and 962 of the cyclase.

DISCUSSION

This paper is a detailed molecular description of the biochemistry of a new Ca^{2+}-modulated membrane ROS-GC1 signal transduction pathway. The novelty of the pathway is based on the discovery that the Ca^{2+} sensor neurocalcin δ is functionally interlocked with the ROS-GC1 transduction machinery in the specified regions of retinal neurons. With this finding, neurocalcin δ becomes the fourth natural Ca^{2+} sensor modulator of ROS-GC1. The other three are the two GCAPs, 1 and 2, and S100β. The neurocalcin δ-modulated ROS-GC1 signal transduction pathway becomes a new paradigm of Ca^{2+} signaling in the retinal neurons.

Neurocalcin δ has been purified from the IPL of the retinal neurons and characterized on the basis of the sequence of its internal fragments. The sequencing failed with the intact native protein, indicating that its N-terminus is blocked, and the protein is acylated in its native state. Mass spectral analyses showed that the acyl group is the myristoyl group. This identifies the native IPL protein as myr-neurocalcin δ. Consistent with this conclusion, the sequence of the cloned form of the protein shows that it contains a consensus site for myristoylation. Except for the Kv channel subfamily, the

FIGURE 9: Neurocalcin δ-binding domain which resides in the ROS-GC1 fragment of amino acids 733−1054 and is distinct from the S100β-binding domain, as studied by direct binding. (A) Dose-dependent stimulation of ROS-GC1 with neurocalcin δ. Membranes were isolated from COS cells expressing wt-r ROS-GC1. The cDNA fragment encoding the ROS-GC1 domain of amino acids 733−1054 was amplified by PCR, cloned into the bacterial expression vector, and purified as a His tag fusion protein as described in Experimental Procedures. The guanylate cyclase activity was assayed in the presence of incremental concentrations of neurocalcin δ (bacterially expressed and purified, myristoylated form) and at 10 μM Ca^{2+}. The specific activity, picomoles of cyclic GMP synthesized per minute per milligram of protein, was plotted as a function of the concentration of neurocalcin δ. The experiments were carried out in triplicate and repeated for reproducibility. The results are from one representative experiment. (B) Binding of the ROS-GC1 fragment of amino acids 733−1054 to neurocalcin δ is Ca^{2+}-dependent. For real-time analysis, neurocalcin δ was immobilized on a CM5 chip (BIAcore) and the soluble ROS GC-1 cytosolic domain of amino acids 733−1054 (analyte) was supplied in the mobile phase at 0.5 μM in the presence of Ca^{2+} (2 mM) or in its absence (in the presence of 1 mM EGTA). Overlaid sensorgrams display the binding of the analyte to neurocalcin δ. The curves were obtained after subtracting the effect of buffers and salts on resonance signals using the unimmobilized surface in flow cell 1 as a reference surface. (C) Binding of the ROS-GC1 cytosolic domain of amino acids 733−1054 to neurocalcin δ. For real-time analysis, the soluble ROS GC-1 cytosolic domain of amino acids 733−1054 (analyte) was supplied in the mobile phase at concentrations between 0.1 and 5 μM. Overlaid sensorgrams display the concentration-dependent binding of the analyte to immobilized neurocalcin δ in the presence of 2 mM $CaCl_2$. The concentration of the analyte is indicated alongside the curves. The curves were obtained after subtracting the effect of buffers and salts on resonance signals using the unimmobilized surface in flow cell 1 as a reference surface. (D) Binding of the ROS-GC1 cytosolic domain of amino acids 733−1054 to neurocalcin δ. The binding response at equilibrium (R_{eq}) determined through real-time analysis was plotted as a function of the concentration of the analyte (ROS-GC1 fragment). The half-maximal binding occurred at 500 nM. (E) Binding of the ROS-GC1 cytosolic domain of amino acids 733−1054 to neurocalcin δ. To assess the calcium dependence, real-time binding analyses with neurocalcin δ were carried out using 0.5 μM analyte with incremental calcium concentrations (0−10 μM). The response at equilibrium (R_{eq}) was plotted as a function of Ca^{2+} concentration. Half-maximal binding occurred at 0.1 μM. (F) The neurocalcin δ-binding site on the ROS-GC1 cytosolic domain does not overlap with its S100β-binding sites. The cDNA fragment encoding the ROS-GC1 domain of amino acids 963−1054 was amplified by PCR, cloned into the bacterial expression vector, and purified as a His tag fusion protein. The fragment was immobilized as described in Experimental Procedures. S100β (commercially obtained) or bacterially expressed and purified myr-neurocalcin δ was supplied in the mobile phase at a concentration of 1 μM in the presence of 2 mM Ca^{2+}, and real-time binding was monitored. (G) ROS-GC1 domain (amino acids 733−1054). A schematic diagram of ROS-GC1, with its multiple domains shaded differently, is provided. The leader sequence (L), the transmembrane (TM), the extracellular (EXT), and the intracellular (INT) regions have been identified. The neurocalcin δ-binding domain, which resides between ROS-GC1 amino acids 733 and 963, is denoted.

myristoylation consensus sequence, MGXXXS, at the N-terminus is conserved in all subfamilies of the neuronal Ca^{2+} sensor proteins (reviewed in refs *36* and *37*); with this study, it has been determined that this feature is also present in the IPL neurocalcin δ.

Recoverin is the founding member of the neuronal Ca^{2+} sensor protein family (*40*, *41*; reviewed in ref *45*). It occurs in the membranes of ROS and, therein, inhibits the rhodopsin kinase activity in a millisecond time process of phototransduction (*42*, *58*, *59*). Through comprehensive studies, a role for the myristoyl group has been assigned in recoverin (*39*, *41*, *42*, *44*, *45*, *60*). Once Ca^{2+} binds, the group translocates recoverin from the cytosol to the membrane. The proposed mechanism holds that without Ca^{2+}, the myristoyl group is sequestered within a hydrophobic pocket of the protein in the cytosol. Once Ca^{2+} binds, it is extruded out, which permits it to interact with the lipid bilayer. This mechanism has been confirmed recently (*43*).

The results of this study show that the operational features of the above mechanism are also present in the case of native retinal neurocalcin δ present in the IPL. In the presence of Ca^{2+}, neurocalcin δ exists as a membrane-bound protein, and in the absence of Ca^{2+}, the majority of it, *but not all*, moves into the cytosol.

An important noteworthy fact revealed by this study is that even extensive washing of the native IPL membranes with EGTA does not completely dissociate neurocalcin δ from the membranes. This indicates that a residual fraction of neurocalcin δ is always bound with the native membranes. This conclusion is validated with the studies on the recombinant reconstituted system. In the presence of Ca^{2+}, the recombinant form of the myr-neurocalcin δ incubated with the native membrane fraction of the inner plexiform layer remains membrane-bound, and when Ca^{2+} is removed through the treatment of EGTA, the majority of it, *but not all*, is no longer membrane-bound (Figure 4B). Thus, the recombinant neurocalcin δ in the native membranes of the IPL mimics the Ca^{2+}-dependent mobility and the membrane anchoring profile of the native neurocalcin δ present in the native inner plexiform membranes. There are two possible reasons for the association of neurocalcin δ with the native membranes, and both are related to the concentration of Ca^{2+} in the resting state of the membranes. First, a cellular Ca^{2+} concentration of 100−200 nM is able to keep the neurocalcin δ membrane-bound. Second, when present with its target protein at this concentration of Ca^{2+}, the neurocalcin δ−target protein complex has a stronger affinity for the membranes than does neurocalcin δ alone. Any, or both, of these possibilities suggest that the membrane-bound neurocalcin δ can participate in the Ca^{2+}-dependent events, which occur at millisecond time intervals.

The detailed studies with the brain and reconstituted lipid membranes have already established the role of the Ca^{2+}−myristoyl switch for neurocalcin δ (*31*, *44*). The study presented here is in accord with and extends the conclusions of those findings. It confirms the role of the myristoyl switch for the native IPL membranes, and it also shows that the switch is operative at the resting states of the cellular Ca^{2+} (100−200 nM) in the native IPL.

In common with recoverin and neurocalcin δ, two other neuronal Ca^{2+} sensor proteins, GCAP1 and GCAP2, under native conditions in ROS are also myristoylated (*61*−*64*), and they also function on a millisecond time scale in the operation of phototransduction. The recent studies show that in both of these GCAPs, the Ca^{2+}−myristoyl switch does not operate like recoverin and neurocalcin δ. In GCAP2, the switch appears to function in a reverse fashion: it is membrane-bound in the absence of Ca^{2+} and exists in the cytosol in its presence (*61*). In GCAP1, it has no role in anchoring it to the membrane (*64*); instead, it controls its Ca^{2+}-dependent regulatory properties (*55*, *64*, *65*). This is an important point and is discussed latter to show that the neurocalcin δ Ca^{2+}−myristoyl switch imparts both the membrane anchoring and regulatory properties to the protein.

Earlier reconstitution studies with the recombinant non-myristoylated neurocalcin δ and ROS-GC1 have shown that neurocalcin δ stimulates ROS-GC1 in a Ca^{2+}-dependent manner (*46*). With the finding that neurocalcin δ is present in the native membrane fraction of the IPL of the retina, its natural interaction with ROS-GC1 was envisioned, tested, and found. Both neurocalcin δ and ROS-GC1 are in the proximity of each other which indicates that they interact with each other, and their interaction might be functionally productive. The finding that the added presence of exogenous Ca^{2+} in the IPL membranes stimulates native guanylate cyclase activity reveals that the interaction between neurocalcin δ and the hypothetical cyclase is, indeed, functionally relevant. It also indicates that these membranes contain a sufficient amount of the residual Ca^{2+} to place neurocalcin δ in contact with the membranes. Thus, the role of Ca^{2+} appears to be twofold: (1) in its nanomolar (resting) concentration range, to keep neurocalcin δ membrane-bound; and (2) in its submicromolar to micromolar range, to create the physical and functional interaction between neurocalcin δ and the cyclase.

These findings establish that the myristoylated form of neurocalcin δ is present in the membranes of the IPL and that it physically interacts with ROS-GC1. The findings, however, do not show the direct and specific functional interaction between neurocalcin δ and ROS-GC1. There are three known forms of ROS-GC: ROS-GC1, ROS-GC2, and ONE-GC (reviewed in refs *2* and *19*). Which of the cyclases is linked with neurocalcin δ in the OPL?

To solve this problem, we took advantage of the known biochemical features of ROS-GCs and the existing discriminatory probes against the ROS-GCs. ROS-GC1 is the only cyclase which is stimulated by all four modulators: two GCAPs, S100β, and neurocalcin δ. Neurocalcin δ does not affect the activity of ROS-GC2 (*46*), and GCAPs have no effect on ONE-GC (*25*). The IPL membrane guanylate cyclase responds to all four modulators. Thus, it meets the criteria of being ROS-GC1. Further biochemical analysis of the inner plexiform membrane guanylate cyclase fraction shows that it directly and specifically interacts with neurocalcin δ. The only other membrane guanylate cyclase that senses and responds to the Ca^{2+}-dependent stimulation via neurocalcin δ is ONE-GC [also called GC-D (*66*)], present in the bovine olfactory neuroepithelial layer. However, ONE-GC is not present in the retinal neurons (*66*). It is, thus, concluded that the neurocalcin δ-modulated Ca^{2+} signaling ROS-GC1 transduction machinery is present specifically in the IPL of the retinal neurons.

To have meaningful physiological participation of Ca^{2+} signaling in the neurocalcin δ-modulated ROS-GC1 trans-

duction machinery in the retinal neurons, the machinery must respond and be operated rapidly by the submicromolar to micromolar range of free Ca^{2+} concentrations. The binding constants obtained with SPR studies show that without Ca^{2+}, neurocalcin δ has no affinity for ROS-GC1. In the presence of Ca^{2+}, it binds ROS-GC1 with high affinity with a K_A of 2.3×10^6 M^{-1} and a K_D of 4.6×10^{-7} M. This indicates that neurocalcin δ binding to and dissociation from ROS-GC1 are Ca^{2+}-dependent, direct, and of high affinity, and they occur very rapidly in response to the submicromolar to the micromolar Ca^{2+} fluctuations. Thus, once Ca^{2+} binds, neurocalcin δ undergoes conformational change, as evidenced by the mobility shift assay, and stimulates ROS-GC1. The EC_{50} of Ca^{2+} for the neurocalcin δ-dependent ROS-GC1 activation is $\sim$0.8 μM, and the EC_{50} value of neurocalcin δ for ROS-GC1 stimulation is also $\sim$0.8 μM. Thus, the stimulation of ROS-GC1 by neurocalcin δ occurs within the physiological concentration range of Ca^{2+} and at the physiological concentration of neurocalcin δ. In an earlier publication, the authors reported an EC_{50} value of 20 μM for Ca^{2+} in the neurocalcin δ-dependent activation of ROS-GC1 (*46*). That value was obtained with the reconstituted system of the nonmyristoylated recombinant form of neurocalcin δ and ROS-GC1. The value requires a revision in this investigation. In the comprehensive study presented here and in the repetition of the old study, the authors find no difference in the EC_{50} values between the nonmyristoylated and myristoylated forms of neurocalcin δ; with both forms, the $K_{1/2}$ for activation of free Ca^{2+} is 0.8$-$1 μM for the neurocalcin δ stimulation of ROS-GC1. The maximal velocity of ROS-GC1 achieved by the myr-neurocalcin δ is, however, $\sim$2-fold higher than that of the nonmyristoylated form (manuscript being prepared). Thus, compared to the nonmyristoylated form, myr-neurocalcin δ is a more productive modulator of ROS-GC1, yet the potency of the two forms is identical. Thus, it is concluded that myristoylation has no effect on the potency of neurocalcin δ; it, however, significantly elevates the V_{max} of ROS-GC1. The primary function of the myristoyl group is to carry neurocalcin δ from the soluble to the membrane portion of the cell. This occurs even in the resting (nanomolar to submicromolar) range of Ca^{2+} concentrations in the neuron. Its secondary function is to respond quickly, in the millisecond range, to additional Ca^{2+} fluctuations. The increments in Ca^{2+} concentration enhance the saturation activity of the cyclase, and the decrements proportionately decrease it. Thus, through its myristoyl group neurocalcin δ acts like recoverin in being anchored to the membranes of the IPL (*39*$-$*43*, *45*) and like GCAPs in regulating ROS-GC1 (*55*, *64*, *65*). These two features together classify neurocalcin δ as a unique member of the neuronal Ca^{2+} sensor protein family, which is a part of the ROS-GC1 transduction machinery in the IPL of the retina. These findings also support the concept that the myristoyl group bestows selectivity in function to the neuronal Ca^{2+} sensor proteins (*37*, *67*).

The next question examined herein was whether ROS-GC1 contains a neurocalcin δ-specific domain. Through deletion and hybrid mutagenesis with the recombinant ROS-GC1, it has been established that the neurocalcin δ-modulated site in ROS-GC1 is separate from the GCAP1-modulated site (*46*). The GCAP1-modulated site has been mapped (*15*). It resides at the N-terminal site juxtaposed to the transmembrane domain in the two small regions, amino acids $M^{445}-L^{456}$ and $L^{503}-I^{522}$, of ROS-GC1 (*15*), and the neurocalcin δ-modulated site resides in the C-terminal region of the cyclase (*46*). The S100β-modulated site also resides in the C-terminal region of ROS-GC1 (*18*). It has also been mapped, and it resides in the two small regions, $Gly^{962}-Asn^{981}$ and $Ile^{1030}-Gln^{1041}$, of the cyclase. The direct binding studies presented here show that neurocalcin δ has no affinity for the S100β sites. Thus, the neurocalcin δ-modulated Ca^{2+} signaling of ROS-GC1 occurs through a domain that is separate from the GCAP- and S100β-modulated domains; it resides within the segment of amino acids 732$-$962, and the domain is neurocalcin δ-specific.

With regard to the physiological linkage of the neurocalcin δ/ROS-GC1 transduction pathway with the activity of a specific retinal neuron, it can be categorically stated that the pathway is not present in the outer segments of the rods and cones. Thus, it is not linked with the phototransduction machinery. In the initial survey of the retina, the study shows that both neurocalcin δ and ROS-GC1 are present in the lower strata of the IPL and a subpopulation of ganglion cells, and provides a strong argument that the pathway is biologically relevant to the physiology of these cellular compartments. Guided by the knowledge gained from the studies in photoreceptors, we predict that the modulation of Ca^{2+} impulses in these neurons via the neurocalcin δ-dependent ROS-GC1 transduction pathway will result in the elevation of the level of cyclic GMP, which, in turn, via a hypothetical CNG channel will depolarize their membranes. This hypothesis deserves serious consideration in its operational applicability in the ganglion neurons. Modeled after the hypothesis, the future work will bring us a step closer in explaining the visual transduction process at a molecular level.

There is one other significant aspect of this study. The study underscores the universality of the emerging concept which predicts that the ROS-GC transduction machinery may be linked with the Ca^{2+} signal transduction processes of all sensory neurons (reviewed in ref *19*). The recent studies and this study show that the machinery is present in the ROS (reviewed in ref *2*), cones (pedicles) (*17*), the photoreceptor$-$bipolar synapse (*18*), the pinealocytes (*23*), the olfactory neuroepithelium (*25*), and the olfactory bulb (*24*). The varying composition of the machinery defines its operational specificity toward being stimulated or inhibited by the Ca^{2+} impulses. When ROS-GC is present with the GCAP modulators, it is inhibited, and when it is present with S100β or neurocalcin δ, it is stimulated. In this manner, it is inhibited in ROS (reviewed in ref *2*), in the cone pedicles, and in the olfactory bulb neurons. However, in the photoreceptor$-$bipolar synapse region, it is stimulated (*18*). In the olfactory neuroepithelium region, it occurs in the form of neurocalcin/ONE-GC, and is stimulated by the Ca^{2+} impulses (*25*). ONE-GC is a variant form of ROS-GC, which does not exist in the retinal neurons (*66*), and so far has been reported to exist solely in the sensory neurons of the olfactory neuroepithelial layer, the site of odorant transduction (*25*, *66*). In contrast to ROS-GC, ONE-GC is only stimulated by the Ca^{2+} impulses, and its natural Ca^{2+} modulator is only neurocalcin δ (*25*). With the study presented here, we conclude that neurocalcin δ is a natural Ca^{2+} modulator of two ROS-GCs: ROS-GC1 and ONE-GC. With ONE-GC, it appears

to be linked with the odorant transduction machinery, and with ROS-GC1, it appears to be linked with the IPL machinery. These illustrations show that with the change in its composition, the ROS-GC transduction machinery achieves universality, cellular specificity, and variability in its operation by the Ca^{2+} signals generated in a wide variety of neurons: retinal, olfactory, pineal, and others to be identified.

ACKNOWLEDGMENT

We thank Dr. J. I. Gordon for the yeast *N*-myristoyltransferase construct, Dr. K. H. Braunewell for the sample of bacterially expressed recombinant VILIP-1, and Dr. P. MacLeish for the 7G6 antibody. We thank Dr. Noga Vardi at the University of Pennsylvania (Philadelphia, PA), in whose laboratory the immunohistochemical analyses were carried out. We thank Joan Sharma for editorial assistance.

REFERENCES

1. Pugh, E. N., Jr., Duda, T., Sitaramayya, A., and Sharma, R. K. (1997) Photoreceptor guanylate cyclases: a review, *Biosci. Rep. 17*, 429−473.
2. Koch, K.-W., Duda, T., and Sharma, R. K. (2002) Photoreceptor specific guanylate cyclases in vertebrate phototransduction, *Mol. Cell. Biochem. 230*, 97−106.
3. Koch, K.-W. (1991) Purification and identification of photoreceptor guanylate cyclase, *J. Biol. Chem. 266*, 8634−8637.
4. Hayashi, F., and Yamazaki, A. (1991) Polymorphism in purified guanylate cyclase from vertebrate rod photoreceptors, *Proc. Natl. Acad. Sci. U.S.A. 88*, 4746−4750.
5. Aparicio, J. G., and Applebury, M. L. (1995) The bovine photoreceptor outer segment guanylate cyclase: purification, kinetic properties, and molecular size, *Protein Expression Purif. 6*, 501−511.
6. Margulis, A., Goraczniak, R. M., Duda, T., Sharma, R. K., and Sitaramayya, A. (1993) Structural and biochemical identity of retinal rod outer segment membrane guanylate cyclase, *Biochem. Biophys. Res. Commun. 194*, 855−861.
7. Goraczniak, R. M., Duda, T., Sitaramayya, A., and Sharma, R. K. (1994) Structural and functional characterization of the rod outer segment membrane guanylate cyclase, *Biochem. J. 302*, 455−461.
8. Duda, T., Goraczniak, R. M., Surgucheva, I., Rudnicka-Nawrot, M., Gorczyca, W. A., Palczewski, K., Baehr, W., and Sharma, R. K. (1996) Calcium modulation of bovine photoreceptor guanylate cyclase, *Biochemistry 35*, 8478−8482.
9. Laura, R. P., Dizhoor, A. M., and Hurley, J. B. (1996) The membrane guanylyl cyclase, retinal guanylyl cyclase-1, is activated through its intracellular domain, *J. Biol. Chem. 271*, 11646−11651.
10. Shyjan, A. W., de Sauvage, F. J., Gillett, N. A., Goeddel, D. V., and Lowe, D. G. (1992) Molecular cloning of a retina-specific membrane guanylyl cyclase, *Neuron 9*, 727−737.
11. Yang, R. B., Foster, D. C., Garbers, D. L., and Fulle, H. J. (1995) Two membrane forms of guanylyl cyclase found in the eye, *Proc. Natl. Acad. Sci. U.S.A. 92*, 602−606.
12. Goraczniak, R. M., Duda, T., and Sharma, R. K. (1998) Calcium modulated signaling site in type 2 rod outer segment membrane guanylate cyclase (ROS-GC2), *Biochem. Biophys. Res. Commun. 245*, 447−453.
13. Lowe, D. G., Dizhoor, A. M., Liu, K., Gu, Q., Spencer, M., Laura, R., Lu, L., and Hurley, J. B. (1995) Cloning and expression of a second photoreceptor-specific membrane retina guanylyl cyclase (RetGC), RetGC-2, *Proc. Natl. Acad. Sci. U.S.A. 92*, 5535−5539.
14. Krishnan, A., Goraczniak, R. M., Duda, T., and Sharma, R. K. (1998) Third calcium-modulated rod outer segment membrane guanylate cyclase transduction mechanism, *Mol. Cell. Biochem. 178*, 251−259.
15. Lange, C., Duda, T., Beyermann, M., Sharma, R. K., and Koch, K.-W. (1999) Regions in vertebrate photoreceptor guanylyl cyclase ROS-GC1 involved in Ca^{2+}-dependent regulation by guanylyl cyclase-activating protein GCAP-1, *FEBS Lett. 460*, 27−31.
16. Krylov, D. M., and Hurley, J. B. (2001) Identification of proximate regions in a complex of retinal guanylyl cyclase 1 and guanylyl cyclase-activating protein-1 by a novel mass spectrometry-based method, *J. Biol. Chem. 276*, 30648−30654.
17. Venkataraman, V., Duda, T., Vardi, N., Koch, K.-W., and Sharma, R. K. (2003) Calcium-modulated guanylate cyclase transduction machinery in the photoreceptor-bipolar synaptic region, *Biochemistry 42*, 5640−5648.
18. Duda, T., Koch, K.-W., Venkataraman, V., Lange, C., Beyermann, M., and Sharma, R. K. (2002) Ca^{2+} sensor S100β-modulated sites of membrane guanylate cyclase in the photoreceptor-bipolar synapse, *EMBO J. 21*, 2547−2556.
19. Sharma, R. K. (2002) Evolution of the membrane guanylate cyclase transduction system, *Mol. Cell. Biochem. 230*, 3−30.
20. Tsien, R. Y. (1981) A non-disruptive technique for loading calcium buffers and indicators into cells, *Nature 290*, 527−528.
21. Redburn, D. A., and Thomas, T. N. (1979) Isolation of synaptosomal fractions from rabbit retina, *J. Neurosci. Methods 1*, 235−242.
22. Zozulya, S., Ladant, D., and Stryer, L. (1995) Expression and characterization of calcium-myristoyl switch proteins, *Methods Enzymol. 250*, 383−393.
23. Venkataraman, V., Nagele, R., Duda, T., and Sharma, R. K. (2000) Rod outer segment membrane guanylate cyclase type 1-linked stimulatory and inhibitory calcium signaling systems in the pineal gland: biochemical, molecular, and immunohistochemical evidence, *Biochemistry 39*, 6042−6052.
24. Duda, T., Venkataraman, V., Krishnan, A., Nagele, R. G., and Sharma, R. K. (2001) Negatively calcium-modulated membrane guanylate cyclase signaling system in the rat olfactory bulb, *Biochemistry 40*, 4654−4662.
25. Duda, T., Jankowska, A., Venkataraman, V., Nagele, R. G., and Sharma, R. K. (2001) A novel calcium-regulated membrane guanylate cyclase transduction system in the olfactory neuroepithelium, *Biochemistry 40*, 12067−12077.
26. Sambrook, M. J., Fritsch, E. F., and Maniatis, T. (1989) *Molecular Cloning: A Laboratory Manual*, Cold Spring Harbor Laboratory Press, Plainview, NY.
27. Paul, A. K., Marala, R. B., Jaiswal, R. K., and Sharma, R. K. (1987) Coexistence of guanylate cyclase and atrial natriuretic factor receptor in a 180-kD protein, *Science 235*, 1224−1226.
28. Nambi, P., Aiyar, N. V., and Sharma, R. K. (1982) Adrenocorticotropin-dependent particulate guanylate cyclase in rat adrenal and adrenocortical carcinoma: Comparison of its properties with soluble guanylate cyclase and its relationship with ACTH-induced steroidogenesis, *Arch. Biochem. Biophys. 217*, 638−646.
29. Burgess, W. H., Jemiolo, D. K., and Kretsinger, R. H. (1980) Interaction of calcium and calmodulin in the presence of sodium dodecyl sulfate, *Biochim. Biophys. Acta 623*, 257−270.
30. Frins, S., Bonigk, W., Muller, F., Kellner, R., and Koch, K.-W. (1996) Functional characterization of a guanylyl cyclase-activating protein from vertebrate rods. Cloning, heterologous expression, and localization, *J. Biol. Chem. 271*, 8022−8027.
31. Ladant, D. (1995) Calcium and membrane binding properties of bovine neurocalcin delta expressed in *Escherichia coli*, *J. Biol. Chem. 270*, 3179−3185.
32. Okazaki, K., Watanabe, M., Ando, Y., Hagiwara, M., Terasawa, M., and Hidaka, H. (1992) Full sequence of neurocalcin, a novel calcium-binding protein abundant in central nervous system, *Biochem. Biophys. Res. Commun. 185*, 147−153.
33. Wang, W., Zhou, Z., Zhao, W., Huang, Y., Tang, R., Ying, K., Xie, Y., and Mao, Y. (2001) Molecular cloning, mapping and characterization of the human neurocalcin delta gene (NCALD), *Biochim. Biophys. Acta 1518*, 162−167.
34. Terasawa, M., Nakano, A., Kobayashi, R., and Hidaka, H. (1992) Neurocalcin: a novel calcium-binding protein from bovine brain, *J. Biol. Chem. 267*, 19596−19599.
35. Vijay-Kumar, S., and Kumar, V. D. (1999) Crystal structure of recombinant bovine neurocalcin, *Nat. Struct. Biol. 6*, 80−88.
36. Braunewell, K. H., and Gundelfinger, E. D. (1999) Intracellular neuronal calcium sensor proteins: a family of EF-hand calcium-binding proteins in search of a function, *Cell Tissue Res. 295*, 1−12.
37. Burgoyne, R. D., and Weiss, J. L. (2001) The neuronal calcium sensor family of Ca^{2+}-binding proteins, *Biochem. J. 353*, 1−12.
38. Nakano, A., Terasawa, M., Watanabe, M., Usuda, N., Morita, T., and Hidaka, H. (1992) Neurocalcin, a novel calcium binding protein with three EF-hand domains, expressed in retinal amacrine cells and ganglion cells, *Biochem. Biophys. Res. Commun. 186*, 1207−1211.

39. Zozulya, S., and Stryer, L. (1992) Calcium-myristoyl protein switch, *Proc. Natl. Acad. Sci. U.S.A. 89*, 11569−11573.
40. Tanaka, T., Ames, J. B., Harvey, T. S., Stryer, L., and Ikura, M. (1995) Sequestration of the membrane-targeting myristoyl group of recoverin in the calcium-free state, *Nature 376*, 444−447.
41. Hughes, R. E., Brzovic, P. S., Klevit, R. E., and Hurley, J. B. (1995) Calcium-dependent solvation of the myristoyl group of recoverin, *Biochemistry 34*, 11410−11416.
42. Senin, I. I., Vaganova, S. A., Weiergraber, O. H., Ergorov, N. S., Philippov, P. P., and Koch, K.-W. (2003) Functional restoration of the Ca^{2+}-myristoyl switch in a recoverin mutant, *J. Mol. Biol. 330*, 409−418.
43. Valentine, K. G., Mesleh, M. F., Opella, S. J., Ikura, M., and Ames, J. B. (2003) Structure, topology, and dynamics of myristoylated recoverin bound to phospholipid bilayers, *Biochemistry 42*, 6333−6340.
44. Beven, L., Adenier, H., Kichenama, R., Homand, J., Redeker, V., Le Caer, J. P., Ladant, D., and Chopineau, J. (2001) Ca^{2+}-myristoyl switch and membrane binding of chemically acylated neurocalcins, *Biochemistry 40*, 8152−8160.
45. Ames, J. B., Tanaka, T., Stryer, L., and Ikura, M. (1996) Portrait of a myristoyl switch protein, *Curr. Opin. Struct. Biol. 6*, 432−438.
46. Kumar, V. D., Vijay-Kumar, S., Krishnan, A., Duda, T., and Sharma, R. K. (1999) A second calcium regulator of rod outer segment membrane guanylate cyclase, ROS-GC1: neurocalcin, *Biochemistry 38*, 12614−12620.
47. Liu, X., Seno, K., Nishizawa, Y., Hayashi, F., Yamazaki, A., Matsumoto, H., Wakabayashi, T., and Usukura, J. (1994) Ultrastructural localization of retinal guanylate cyclase in human and monkey retinas, *Exp. Eye Res. 59*, 761−768.
48. Cooper, N., Liu, L., Yoshida, A., Pozdnyakov, N., Margulis, A., and Sitaramayya, A. (1995) The bovine rod outer segment guanylate cyclase, ROS-GC, is present in both outer segment and synaptic layers of the retina, *J. Mol. Neurosci. 6*, 211−222.
49. Margulis, A., Pozdnyakov, N., and Sitaramayya, A. (1996) Activation of bovine photoreceptor guanylate cyclase by S100 proteins, *Biochem. Biophys. Res. Commun. 218*, 243−247.
50. Pozdnyakov, N., Goraczniak, R., Margulis, A., Duda, T., Sharma, R. K., Yoshida, A., and Sitaramayya, A. (1997) Structural and functional characterization of retinal calcium-dependent guanylate cyclase activator protein (CD-GCAP): identity with S100β protein, *Biochemistry 36*, 14159−14166.
51. Duda, T., Goraczniak, R. M., and Sharma, R. K. (1996) Molecular characterization of S100A1-S100B protein in retina and its activation mechanism of bovine photoreceptor guanylate cyclase, *Biochemistry 35*, 6263−6266.
52. Duda, T., Venkataraman, V., Jankowska, A., Lange, C., Koch, K.-W., and Sharma, R. K. (2000) Impairment of the rod outer segment membrane guanylate cyclase dimerization in a cone-rod dystrophy results in defective calcium signaling, *Biochemistry 39*, 12522−12533.
53. Yu, H., Olshevskaya, E., Duda, T., Seno, K., Hayashi, F., Sharma, R. K., Dizhoor, A. M., and Yamazaki, A. (1999) Activation of retinal guanylyl cyclase-1 by Ca^{2+}-binding proteins involves its dimerization, *J. Biol. Chem. 274*, 15547−15555.
54. Ramamurthy, V., Tucker, C., Wilkie, S. E., Daggett, V., Hunt, D. M., and Hurley, J. B. (2001) Interactions within the coiled-coil domain of RetGC-1 guanylyl cyclase are optimized for regulation rather than for high affinity, *J. Biol. Chem. 276*, 26218−26229.
55. Hwang, J. Y., Lange, C., Helten, A., Hoppner-Heitmann, D., Duda, T., Sharma, R. K., and Koch, K.-W. (2003) Regulatory modes of rod outer segment membrane guanylate cyclase differ in catalytic efficiency and Ca^{2+}-sensitivity, *Eur. J. Biochem. 270*, 3814−3821.
56. Duda, T., and Koch, K.-W. (2002) Calcium-modulated membrane guanylate cyclase in synaptic transmission? *Mol. Cell. Biochem. 230*, 107−116.
57. Sitramayya, A. (2002) Calcium-dependent activation of guanylate cyclase by S100β, *Adv. Exp. Med. Biol. 514*, 389−398.
58. Kawamura, S., Hisatomi, O., Kayada, S., Tokunaga, F., and Kuo, C. H. (1993) Recoverin has S-modulin activity in frog rods, *J. Biol. Chem. 268*, 14579−14582.
59. Senin, I. I., Zargarov, A. A., Alekseev, A. M., Gorodovikova, E. N., Lipkin, V. M., and Philippov, P. P. (1995) N-Myristoylation of recoverin enhances its efficiency as an inhibitor of rhodopsin kinase, *FEBS Lett. 376*, 87−90.
60. Ames, J. B., Ishima, R., Tanaka, T., Gordon, J. I., Stryer, L., and Ikura, M. (1997) Molecular mechanics of calcium-myristoyl switches, *Nature 389*, 198−202.
61. Olshevskaya, E. V., Hughes, R. E., Hurley, J. B., and Dizhoor, A. M. (1997) Calcium binding, but not a calcium-myristoyl switch, controls the ability of guanylyl cyclase-activating protein GCAP-2 to regulate photoreceptor guanylyl cyclase, *J. Biol. Chem. 272*, 14327−14333.
62. Otto-Bruc, A., Buczylko, J., Surgucheva, I., Subbaraya, I., Rudnicka-Nawrot, M., Crabb, J. W., Arendt, A., Hargrave, P. A., Baehr, W., and Palczewski, K. (1997) Functional reconstitution of photoreceptor guanylate cyclase with native and mutant forms of guanylate cyclase-activating protein 1, *Biochemistry 36*, 4295−5302.
63. Schrem, A., Lange, C., Beyermann, M., and Koch, K.-W. (1999) Identification of a domain in guanylyl cyclase-activating protein 1 that interacts with a complex of guanylyl cyclase and tubulin in photoreceptors, *J. Biol. Chem. 274*, 6244−6249.
64. Hwang, J. Y., and Koch, K.-W. (2002) Calcium- and myristoyl-dependent properties of guanylate cyclase-activating protein-1 and protein-2, *Biochemistry 41*, 13021−13028.
65. Hwang, J. Y., and Koch, K.-W. (2002) The myristoylation of the neuronal Ca^{2+}-sensors guanylate cyclase-activating protein 1 and 2, *Biochim. Biophys. Acta 1600*, 111−117.
66. Fulle, H. J., Vassar, R., Foster, D. C., Yang, R. B., Axel, R., and Garbers, D. L. (1995) A receptor guanylyl cyclase expressed specifically in olfactory sensory neurons, *Proc. Natl. Acad. Sci. U.S.A. 92*, 3571−3575.
67. O'Callaghan, D. W., Ivings, L., Weiss, J. L., Ashby, M. C., Tepikin, A. V., and Burgoyne, R. D. (2002) Differential use of myristoyl groups on neuronal calcium sensor proteins as a determinant of spatio-temporal aspects of Ca^{2+} signal transduction, *J. Biol. Chem. 277*, 14227−14237.

BI035631V